

AD-A144 559

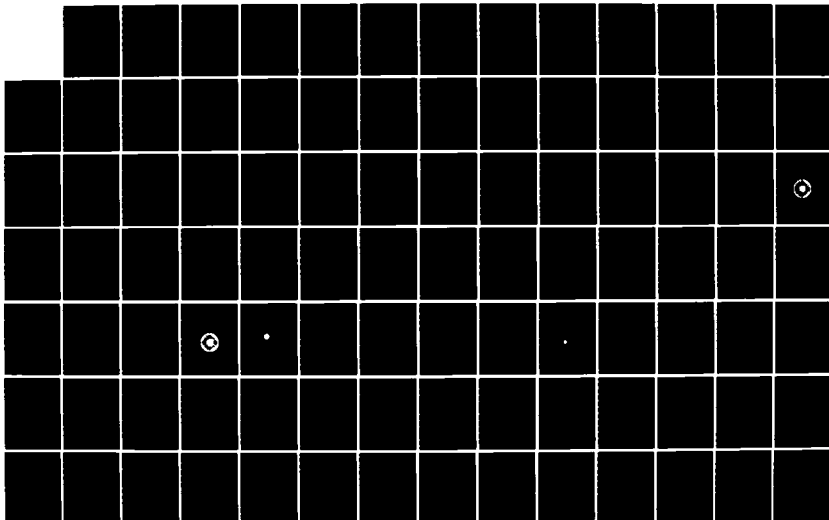
COMPUTER AIDED GEOMETRICAL OPTICS DESIGN(U) AIR FORCE  
INST OF TECH WRIGHT-PATTERSON AFB OH SCHOOL OF  
ENGINEERING D J TIPPLE DEC 83 AFIT/GEP/PH/83D-14

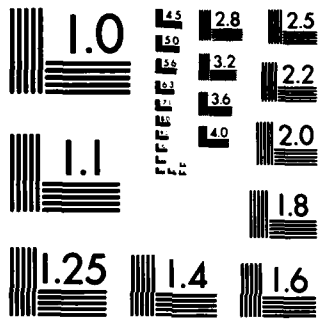
1/2

UNCLASSIFIED

F/G 20/6

NL





MICROCOPY RESOLUTION TEST CHART  
NATIONAL BUREAU OF STANDARDS-1963-A

AD-A144 559

DTIC FILE COPY



COMPUTER AIDED GEOMETRICAL  
OPTICS DESIGN  
THESIS

DONALD J. TIPPLE

AFIT/GEP/PH/83D-14

Capt

USAF

This document has been approved  
for public release and its  
distribution is unlimited.

REC 24 104

DEPARTMENT OF THE AIR FORCE  
AIR UNIVERSITY

**AIR FORCE INSTITUTE OF TECHNOLOGY**

Wright-Patterson Air Force Base, Ohio

84 08 20 088

AFIT/GEP/PH/83D-14

COMPUTER AIDED GEOMETRICAL  
OPTICS DESIGN  
THESIS

DONALD J. TIPPLE

AFIT/GEP/PH/83D-14    Capt    USAF

Approved for public release; distribution unlimited

AFIT/GEP/PH/83D-14

COMPUTER AIDED GEOMETRICAL OPTICS DESIGN

THESIS

Presented to the Faculty of the School of Engineering  
of the Air Force Institute of Technology  
Air University  
in Partial Fulfillment of the  
Requirement for the Degree of  
Master of Science

by

Donald J. Tipple, BA

Captain USAF

Graduate Engineering Physics

December 1983



A-1

Approved for public release; distribution unlimited

## Preface

7-2-15  
The purpose of this study was to employ the FALCON optical design computer program to accomplish the design and analysis of a complex optical system. To this end, a working knowledge of the code, its capabilities, its limitations, and of optical design techniques were all gained. ✓

I wish to thank Lt Col John Erkkila for acting as my advisor, for sharing my triumphs and tragedies throughout the entire project, and for his guidance and counsel. In addition, I wish to thank Dr John Loomis of the University of Dayton for sharing with me his expertise as the author of the FALCON code. I also wish to thank Captains William Welker and Michael Wahlstedt whose advice and theses aided greatly. Lastly, I wish to thank my wife, June, for her unfailing support and ever present optimism.

Donald J. Tipple

## CONTENTS

	Page
Preface.....	ii
List of Figures.....	iv
List of Tables.....	vi
Abstract.....	vii
I. Introduction.....	1
Problem.....	2
Assumptions.....	2
Approach.....	3
II. The FALCON Program.....	5
Optical System Input.....	7
Evaluation Command.....	15
Graphics Commands.....	20
Lens Library.....	32
III. Triplet Evaluation.....	33
Manual Ray Tracing.....	35
Achromatic Aberrations.....	39
Triplet Evaluation Using FALCON Code.....	43
IV. The Design Problem: Off-Axis Beam Expander...	59
V. Conclusion.....	80
Triplet Analysis.....	80
Off-Axis Beam Expander.....	81
Recommendations.....	82
Bibliography.....	84
Appendix I: Glossary.....	86
Appendix II: Running FALCON.....	87
Appendix III: Diffraction Theory of Aberrations...	89
Appendix IV: Zernike Polynomials.....	102
Appendix V: Basic Program Listing.....	104
Vita.....	105

## List of Figures

Figure		Page
2-1	Falcon Coordinates and Symbology.....	6
2-2	Single Thin Lens Input Example.....	9
2-3	Euler Angles.....	14
2-4	Tilt and Decenter Operations.....	14
2-5	LEPRT Command Output.....	16
2-6	OCON Command Output.....	16
2-7	PARAX Command Output.....	17
2-8	FORD Command Output.....	18
2-9	ZPOLY Command Output.....	21
2-10	LAYOUT Command Output.....	23
2-11	Radial Energy Distribution Plot.....	24
2-12	Knife Edge Distribution Plot.....	26
2-13	Wavefront Contour Plot.....	27
2-14	Isometric Wavefront Plot.....	28
2-15	Fan Plots.....	30
2-16	Spot Plot.....	31
3-1	Cooke Triplet.....	35
3-2	Ray Trace Table (First Section).....	35
3-3	Ray Trace Table (Second Section).....	36
3-4	Ray Trace Table (Third Section).....	37
3-5	Tangential and Sagittal Planes.....	39
3-6	Wavefront Aberration Function Parameters.....	41
3-7	Seidel Coefficients.....	43
3-8	Falcon Lens Specification - Cooke Triplet.....	44

Figure	Page
3-9 ZPOLY LIST Output.....	46
3-10 Spot Diagram for Original Triplet.....	49
3-11 Spot Diagram for Adjusted Triplet.....	50
3-12 Wavefront Contour Plot for Original Triplet...	52
3-13 Wavefront Contour Plot for Adjusted Triplet...	53
3-14 Isometric Wavefront Plot for Original Triplet.	54
3-15 Isometric Wavefront Plot for Adjusted Triplet.	54
3-16 Spot Diagram for Adjusted Triplet.....	55
3-17 Contour Wavefront Plot for Decentered Triplet.	56
3-18 Isometric Wavefront Plot for Decentered Triplet.....	57
4-1 Beam Expander System Layout.....	62
4-2 Tilts and Decenters.....	70
4-3 ZPOLY LIST Output Summary.....	75
4-4 Wavefront Contour Plot.....	77
4-5 Isometric Wavefront Plot.....	78
4-6 Spot Diagram.....	79

## List of Tables

Table		Page
3-1	Triplet Intersurface Distance.....	48
3-2	Triplet Aberrations and Strehl Ratio.....	49
4-1	Preliminary Design Solutions.....	66
4-2	Paraxial Output Beam Parameters.....	67
4-3	Aberrations and Strehl Ratios.....	68
4-4	Beam Expander Input.....	69

Abstract

The FALCON optical design and evaluation computer program was examined and applied to two efforts. The first effort involved the evaluation of a Cooke triplet and manual verification of some of the code's results. The second effort was the design of a beam expander, the function of which is to expand and square a high aspect ratio rectangular laser beam. The system uses a single spherical mirror and two cylindrical mirrors to produce the desired output. A brief discussion of the diffraction theory of aberrations and aberration balancing gives some of the basis upon which the FALCON code is constructed.

## I. INTRODUCTION

### Background

Prior to 1930 all lenses were designed using logarithms, and from 1930 to about 1960 they were designed by hand using mechanical desk calculators and sine tables (Ref 1:58). This was a long and tedious process because the design of optical systems is, in general, an iterative process requiring a "first guess" followed by successive refinements to eventually arrive at an acceptable design. The iterative approach is still used, however, enhanced through the use of the modern digital computer.

The iterative approach is applied to two different design/evaluation problems. The first problem demonstrates the FALCON optical design program by evaluating the design of a Cooke triplet. This is intended to be used as a pedagogical exercise to familiarize the reader with the use of several of the commands, outputs, and features of the Falcon program. Some computer generated results are manually verified to add credibility and understanding to the internal workings of the FALCON program.

The second design problem involves a three-mirror beam expander system employing one spherical and two cylindrical elements to square a rectangular input. This design was proposed for study by the Air Force Weapons Laboratory (AFWL). The beam expander is part of a tentative design for

a continuous wave carbon dioxide ring laser. The beam expander will accept the output of the carbon dioxide gain cell in the form of a 1.5 cm by 15 cm rectangular beam. The rectangular beam will be squared by the beam expander to 12 cm by 12 cm. The square beam will then be directed through a scraper to remove a 1.5 cm by 12 cm portion and, to complete the ring, this rectangular beam will be directed into the gain cell.

#### Problem

The problem is divided into two segments. The first problem segment involves becoming familiar with the features, capabilities, limitations, and operation of the FALCON optical design program. To this end, a relatively simple optical system is evaluated using FALCON and the results are compared with available published values. A Cooke triplet is used as the subject system due to its relative simplicity and the availability of published data.

The second problem segment involves evaluating an off-axis reflective beam expander design proposed by AFWL, the purpose of which is to square a high aspect ratio rectangular laser beam input into the system. The system, as proposed, employs two cylindrical elements and a single spherical element. The problem requires the development of a design and its subsequent evaluation.

#### Assumptions

For the first problem segment, it was assumed that the

published values for the triplet being evaluated are correct. For the second problem segment, it was assumed that the FALCON program was operating correctly. Furthermore, from pragmatic considerations, the linear dimension of the beam expander will not exceed six meters in length. Since the beam expander is to be used with a laser beam with a wavelength of 10.6 microns, the effects of chromatic aberrations are not considered. In addition, the FALCON code uses Zernike polynomials to calculate wavefront aberrations. Zernike polynomials are defined on the unit circle. For exitpupil geometries other than circular, presumably the FALCON code uses an inscribed circle on which the Zernike polynomials are defined thus rendering the use of Zernike polynomials a valid approach for calculating wavefront aberrations.

#### Approach

For the first problem segment, a triplet system was chosen for evaluation whose system specifications were readily available. The specifications were converted into a form suitable for entry into the FALCON program. The triplet system performance was evaluated using FALCON, and in the process, several of the features of the program were demonstrated. Some of the results generated by the FALCON program were then manually verified to add credibility and understanding to the internal workings of the code.

For the second problem segment, the FALCON code was used to evaluate a proposed beam expander design. Insofar as the initially proposed design proved inadequate, the iterative approach was taken to yield an alternative design consistent with the assumptions made above.

## II. THE FALCON PROGRAM

The FALCON optical design and evaluation program was written by Dr. John Loomis while he was a student at the Optical Sciences Center, University of Arizona during the period from 1975 to 1980 (Ref 2:1). The program is written in Fortran for use on Control Data Corporation (CDC) Cyber computers. It may be used in either an interactive or a batch environment using any suitable input, however, in interactive mode there are graphics routines in FALCON that are written for use with Tektronix graphics terminals (nominally Tektronix 4025).

FALCON consists of a number of program segments that are called by the user through commands. The program is capable of handling a wide variety of optical systems, the components of which may consist of spherics, torics, conics, higher order aspherics, diffraction gratings, and Fresnel lenses, all of which may be either transmissive or reflective. Surface tilts and decentering of components can also be accommodated.

Evaluation techniques used by FALCON include paraxial and real ray tracing, calculation of classic third and fifth order ray aberrations, ray fans, spot diagrams, wavefront variance and Strehl ratio determination, radial and knife edge energy distributions, and optical transfer functions (Ref 2:1).

FALCON is a computer program to assist in the evaluation and design of optical systems. It is not an automatic design program. There exists no provision within FALCON to specify a set of acceptable aberration parameters and an approximation to the desired system specification, to allow the program to iteratively refine the design until the acceptable design constraints are met. The somewhat less than automatic nature of the program is not, however, a serious drawback for the novice designer. This is primarily true because without an automatic feature, FALCON forces the novice designer into an understanding of the affects of performing different manipulations on the system. FALCON is therefore intended to assist a designer by providing the appropriate numeric and graphic output to aid the designer in his task.

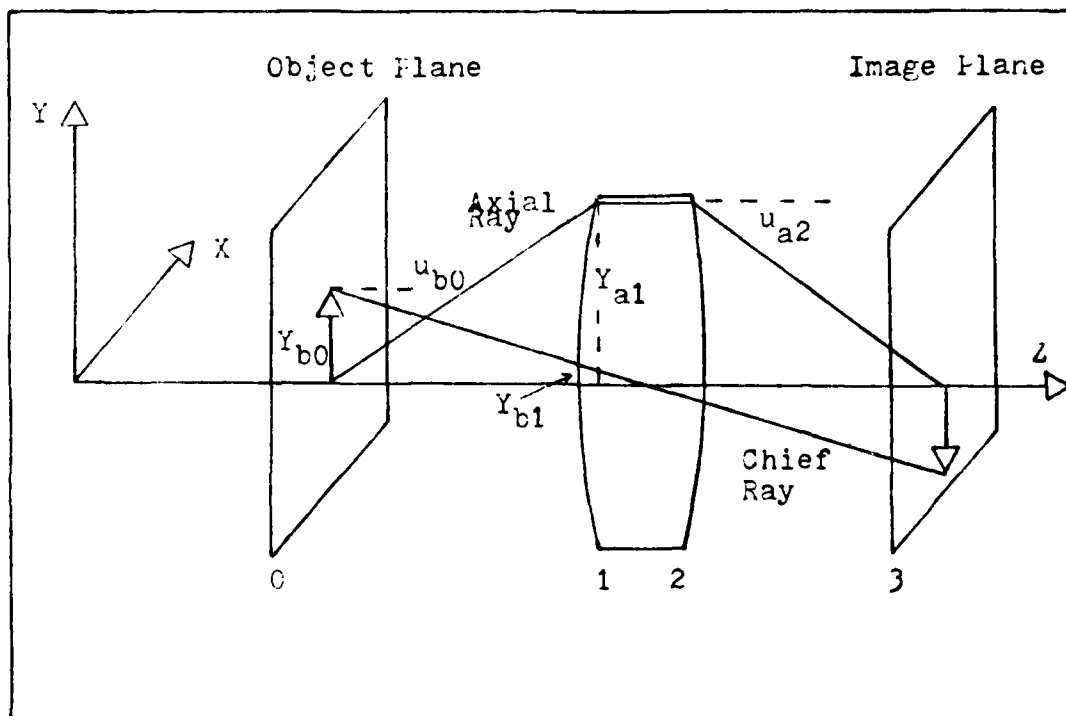


Figure 2-1. FALCON Coordinates and Symbology.

FALCON uses a standard right-handed rectangular coordinate system. Initially, the Z-axis is taken as the optical axis with light propagating in the positive Z direction (from left to right). The coordinate system is shown in Figure 2-1 with some standard symbology used within FALCON.

The notation used is similar to that used by Lea (Ref 5). The subscripts "b" indicate parameters associated with the chief ray. The subscripts "a" relate to the axial ray. The second subscript, an integer, indicates the surface at which a ray is being considered. Distances between surfaces are measured along the optical axis from vertex to vertex or from and to the centers of clear apertures or obstructions. The distance from the object to the first surface can be specified as any distance but if none is specified, the default value is  $10^{10}$  units. The Y-Z plane is taken as the tangential plane. The X-Z plane is taken to be the sagittal plane. These terms are defined in the glossary ( Appendix I). Axial and chief rays are traced in the tangential plane.

#### Optical System Input

A LENS command is used to place FALCON in the mode where it can accept optical system specifications. Next FALCON allows the user to input up to 70 characters of text as a brief description of the system. This single line of text will be used as a caption for graphic output. Each line after the description specifies a surface in the optical system. Surfaces are specified proceeding from left to right

along the Z axis for uniaxial systems. For non-uniaxial systems, the system is specified as light would propagate through the system with the input to the system from the left. In either case the first surface specified is the object surface. This is defined by means of the axial and chief rays. The chief ray may be specified in either of two ways. The first way utilizes the identifier SCY followed by the parameters  $Y_{b0}$  and  $Y_{b1}$  as shown in Figure 2-1.  $Y_{b0}$  is the object height at which the chief ray starts and  $Y_{b1}$  is the height of the chief ray at the first surface. To avoid mistakes, whenever possible it is prudent to specify  $Y_{b0}$  and have the code calculate  $Y_{b1}$ . The second way to specify the chief ray utilizes the YFANG identifier followed by the angle  $u_{b0}$  in degrees followed by  $Y_{b1}$  as before. By omitting  $Y_{b1}$  FALCON calculates the ray height needed at surface 1 to allow the chief ray to pass through the center of the aperture stop. If no aperture stop is specified, the chief ray is then directed to the vertex of surface 1. If a WV is present, up to five wavelengths (measured in microns) may be specified. The first of these wavelengths is taken as the design wavelength. If no WV identifier is present, FALCON defaults to the values 0.58756, 0.48613, 0.65627, 0.43584, and 0.70652 microns for the five wavelengths. The remaining lines are used to specify optical surfaces. This is done by specifying the radius of curvature of that surface preceded by the RD identifier or by specifying the curvature (reciprocal of the radius of curvature) preceded by the CV

identifier. The index of refraction of the medium following the present surface is specified using the GLASS identifier followed by the index of refraction. As an alternative, the refractive index may be specified by choosing a specific type of glass from the Schott glass catalog. Such a catalog, although not complete, is currently installed in the FALCON program. To use this feature, the identifier SCHOTT is used followed by the desired glass type. A single thin lens may be specified to FALCON as shown in Figure 2-2.

```
LENS
LI SINGLE THIN LENS EXAMPLE
SAY 10 SCY -5 TH 50 UNITS CM
CV .01 TH 2 SCHOTT BK7
RD 200 TH 500 GLASS 1.0
END
```

Figure 2-2. Single Thin Lens Input Example

In addition to the refractive surfaces specified in Figure 2-2, there are several other options available. Reflective surfaces are specified by adding the identifier REFL to the line specifying a given surface. A CLAP x y or COBS x y specifies a clear aperture or a central obstruction, respectively. If values for both x and y are included, they specify the x and y semiaxes for an elliptical aperture or obstruction. If the y parameter is excluded, the x value is taken as the radius of a circular aperture. A rectangular

aperture can be specified by including the RECT identifier in addition to using the CLAP or COBS identifier (on the same command line). In this case, the x and y values indicate half of the X and Y dimensions of the rectangle, respectively. If the y parameter is omitted, the aperture is interpreted as a square. A small idiosyncratic error within the program requires the long axis of a rectangular aperture to be aligned in the Y direction. This may, in some cases cause difficulties, however, for the systems considered in this effort, the problem was worked around without difficulty. An ASTOP identifier may also be included to identify the current surface as an aperture stop.

FALCON is capable of handling a host of aspheric surfaces. To identify the current surface as a conic surface of revolution about the optical axis, both the CV identifier and a conic constant must be specified. The conic constant is specified by the CC identifier followed by a parameter k where  $k = -(a^2 - b^2)/a$  where a, and b, are the semimajor and minor axes of the conic surface, respectively (Ref 2:39).

General aspheric coefficients are specified by the ASPH identifier followed by four parameters representing fourth, sixth, eighth, and tenth order surface deformations, respectively. Zero values are assumed for missing coefficients (Ref 2:38).

Toric surfaces have different curvatures in both the tangential and sagittal planes. A general toric surface has an axis of rotation normal to the optical axis. If the axis

of rotation is parallel to the Y axis, the toric is a Y toric, and similarly, if the axis of rotation is parallel to the X axis the toric is an X toric. To identify a surface as a Y toric, the identifier takes the form CVY c', where c' is the curvature of revolution of the surface in the X-Z plane. Similarly, the identifier CVX c specifies an X toric, where c is the curvature of revolution of the surface in the Y-Z plane. Alternatively, the identifiers RDX and RDY can be used to specify X and Y torics, respectively, where the parameter following each is the radius of curvature (1/c' or 1/c). If the curvature of revolution is omitted or specified as zero, the respective toric is a cylinder. Higher order aspherics can be built into toric surfaces by using the ASPH identifier as described earlier.

Paraxial Solves. Written into the FALCON program is a subroutine that makes use of paraxial ray data to calculate either curvatures or distances to produce some desired effect on either the axial or the chief ray angle. The desired result, for example, may be a given ray angle after refraction or a required ray height on the following surface. Solves are available to adjust the curvature of a given surface or the distance between surfaces to achieve this result. The FALCON program has ten solves available for use. These are summarized below (Ref 8:10):

<u>Identifier</u>	<u>Type</u>	<u>Solve</u>	<u>Parameter</u>
PUY	u	Curvature	u is the desired angle after reflection or refraction.

SPY	y	Curvature	y is the desired ray height at the next surface.
PIY	i	Curvature	i is the desired axial ray angle of incidence.
APY		Curvature	Adjusts curvature so $i+u=0$ (the aplanatic condition).
PUCY	u	Curvature	Same as PUY but for chief ray.
SPCY	y	Curvature	Same as SPY but for chief ray.
PICY	i	Curvature	Same as PIY but for chief ray.
PY	y	Thickness	Adjusts distance to next surface so axial ray hits at y.
PCY	y	Thickness	Same as PY but for chief ray.

Paraxial solves are very powerful tools for the designer in that any angle of incidence or refraction can be controlled, or any unknown distance can automatically be determined (Ref 8:11).

Parameter Pickups. Parameter pickups are used to define properties of the current surface in terms of parameters at a different surface. As an example of how this works, the entry NAME, or any other identifier, is included in the input record for a given surface n. The identifier n is stored in

the data block associated with the surface n. By including the entry NAME PICKUP n in the entry for another surface J, it will cause FALCON to scan the data block for the surface n looking for the word NAME. If the word NAME is found, parameters are picked up from that location and used to specify the surface J. The parameter n tells the program which line to look for ( Ref 2:27).

Tilts and Decenters. Tilt and decenter identifiers allow the location and orientation of a given surface to vary with the local coordinate system of the surface. The key here is the LOCAL coordinate system. Decentering is an offset in the local X-Y plane, normal to the optical axis, as defined by the previous surface. The distance between the current surface and the preceding one also enters into the consideration. The TILT function is defined by the Euler angles (in degrees). This allows the coordinate system associated with a surface to be tilted in any or all of three different planes. Positive angles correspond to counterclockwise rotations in the appropriate planes as follows:

X-axis through angle  $\alpha$

New Y-axis through angle  $\beta$

New Z-axis through angle  $\gamma$

This is shown somewhat more clearly in Figure 2-3.

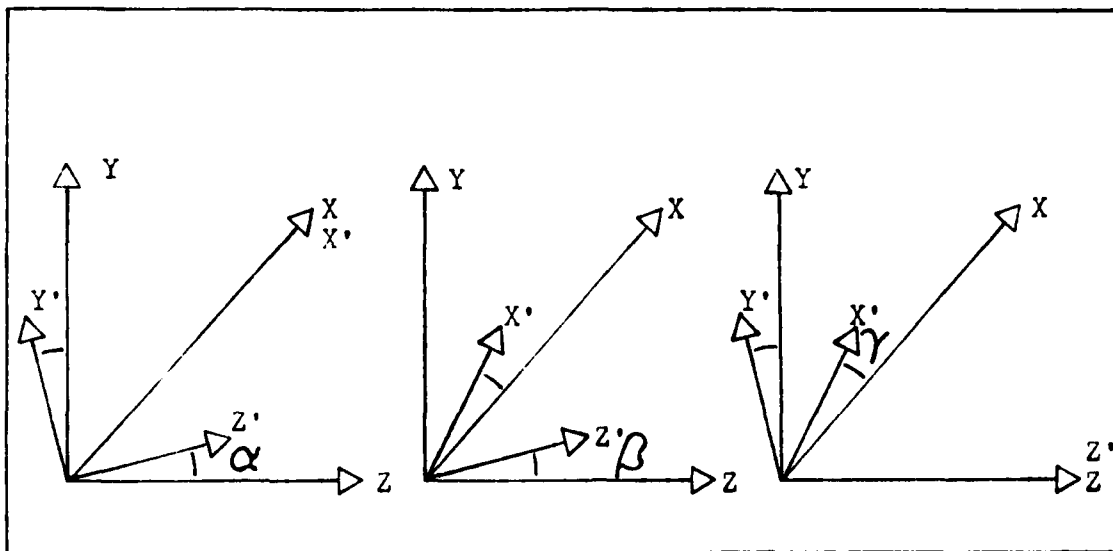


Figure 2-3. Euler Angles

The decenter identifier (DEC  $Y_d$   $X_d$ ) indicates that the local coordinate system for the current surface is to be shifted an amount,  $Y_d$  along the Y-direction and an amount  $X_d$  in the X-direction. Tilt and decenter is shown in Figure 2-4.

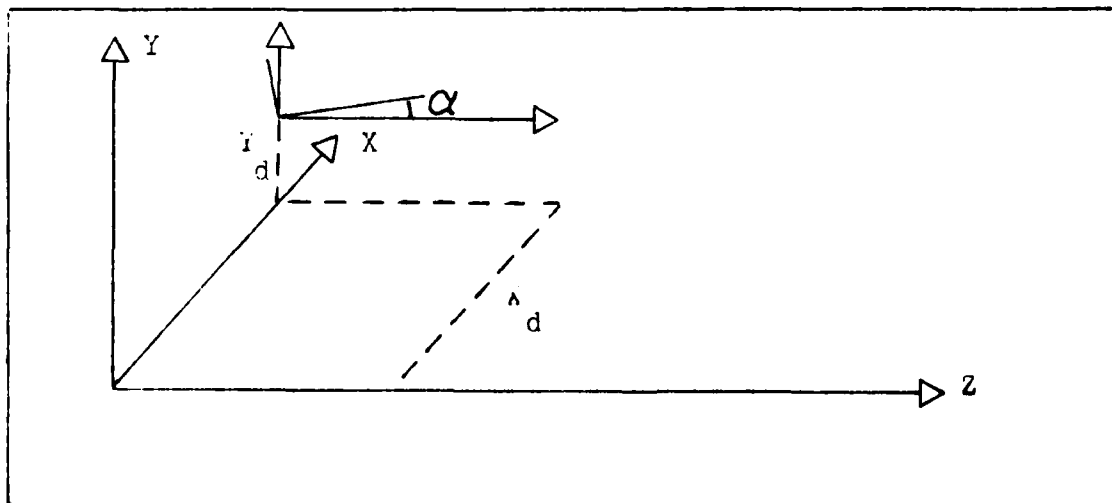


Figure 2-4. Tilt and Decenter Operations.

### Evaluation Commands

After the optical system is specified, FALCON offers several commands to evaluate the system. The outputs resulting from the commands take graphic form, tabular form or a combination of both. Those commands resulting in tabular output are LEPRT, OCON, FORD, RAY, PUPIL, and ZPOLY. These commands along with some of the more useful options are discussed in the following pages.

EFL	BF	F/NBR	LENGTH	OID	T-MAG	
9.9999	14.0502	5.77	3.5523	42.6025	-.577084	
BASIC SYSTEM DATA		UNITS CM				
SURF	CURVATURE	RADIUS	THICKNESS	MEDIUM	INDEX	
0	0.000000	INFINITE	25.000000		1.620000	
1	.252850	3.954914	.600000			
2	-.014740	-67.842605	1.065410			
3	-.199420	-5.014542	.150000		1.621000	
4	.259730	3.850152	1.136910			
5	.050650	19.743337	.600000		1.620000	
6	-.245880	-4.067025	14.050150			
7	0.000000	INFINITE	0.000000			
REFRACTIVE INDICES						
SURF	N1	N2	N3	N4	N5	DF
1	1.620000	1.000000	1.000000	1.000000	1.000000	-1.492
3	1.621000	1.000000	1.000000	1.000000	1.000000	-1.487
5	1.620000	1.000000	1.000000	1.000000	1.000000	-1.492
WVLN	.58756	.48613	.65627	.43584	.70652	

Figure 2-5. LEPRT Command Output

The LEPRT (LEns PRInT) command generates several tables of basic information about the optical system. An example of a typical output from the LEPRT command is shown in Figure 2-5. The first table gives the effective focal length (EFL), the back focal length (BFL), the F number (F/NBR), the axial distance from the first surface to the last surface preceding the image (LENGTH), and the object-to-image distance (OID). The remaining tables are self explanatory.

The LIST command lists all the surfaces specified in the lens deck as specified by the LENS command. The output from this command will appear identical to an optical system previously specified. It is used primarily to view the system parameters prior to editing. See Figure 2-2.

The OCON command provides the same information as the first two lines of the LEPRT output, but in addition, it also identifies the primary surfaces within the system. A typical OCON output is shown in Figure 2-6. The abbreviations used are mnemonically derived from the surfaces that they represent; ER indicates eye relief, EPR denotes the exit pupil radius, A-MAG indicates angular magnification, and LENGTH denotes the distance from the first surface to the surface preceding the image surface.

The PARAX command provides a paraxial ray trace table as its output. It gives ray heights and angles for both chief and axial rays throughout the entire optical system. A sample PARAX output is shown in Figure 2-7.

--OCON

ER	EPR	A-MAG	LENGTH
578.0160	6.0000	-1.25	546.9

XZ PLANE

ER	EPR	A-MAG	LENGTH
17320.3009	6.0068	-.125	546.9

Figure 2-6. OCON Command Output

PARAXIAL TRACE AT WAVELENGTH 1

SURF	AXIAL Y	CHIEF Y	AXIAL U	CHIEF U
0	0.000000	-1.500000	.050000	.060000
1	1.250000	0.000000	-.090098	.037037
2	1.195941	.022222	-.156888	.059797
3	1.028791	.085930	-.018188	.043454
4	1.026063	.092449	.136013	.085350
5	1.180697	.189484	.061071	.049012
6	1.217340	.218891	-.086642	.046030
7	.000000	.865626	-.086642	.046030

Figure 2-7. PARAX Command Output

The FORD command produces an output consisting of third and fifth order ray aberration coefficients. For focal systems, the output is given in the linear units specified in the LENS deck. If a system is designated as AFOCAL, the output is given in radians. These coefficients can, however, be shown to be the classical Seidel coefficients easily

calculated by hand using the forms from Lea (Ref 5:93, 8:14). The output produced by the FORD command are shown in Figure 2-8. The mnemonics below the numeric values indicate the respective parameters. For example, SA3 indicates that the numeric value in the corresponding position is the third order spherical aberration coefficient, measured in centimeters.

Aberration coefficients may be output as unconverted Buchdahl coefficients using the BUCH option after the FORD command. To convert between transverse, Buchdahl and angular coefficients, the following conversion factors  $\mu$  can be used to multiply the FORD BUCH outputs:

- $\mu = 1$  for Buchdahl coefficients
- $\mu = 1/(2n'u')$  for transverse measure
- $\mu = 1/(2n'Yp)$  for angular measure

TRANSVERSE ABERRATIONS AT WAVELENGTH 1				UNITS CM
-.024579	.001375	.000694	-.000123	-.001298
.013922	.009143	.000004	.000000	.000014
.004596	0.000000	0.000000	2.566728	.252110
.000499	.003250	.000741	.001214	.001295
.000302	.000197	.000341	-.000975	
SA3	CMA3	AST3	DIS3	PTZ3
SA 5	CMA5	AST5	DIS5	TPZ5
SA7	PAC	PLC	SAC	SLC
ELCMA	TOBSA	SOBSA	M1	M3
N1	N2	PSA3	PCMA3	

Figure 2-8. FORD Command Output

where  $u'$  and  $n'$  are the ray angle and refractive index, respectively, in image space.  $Y_p$  is the height of the given ray in the exit pupil (Ref 2:64). The RAY command traces an individual ray through the optical system. Ray data are printed for each surface beginning with each surface following the object. The RAY command has the format RAY  $y \ x \ n$ . The parameters  $x$  and  $y$  are fractional reference surface coordinates. Unless otherwise specified, the first surface following the object is the reference surface. The parameter  $n$  is the wavelength number (one through five) specifying the wavelength of the ray to be traced (as defined by the  $wv$  identifier at surface 0, or by default). A table of data for the various optical surfaces will be printed. Ray data are printed for the reference surface and each surface thereafter. The data includes the local coordinates of the ray at the surface, the optical path length of the ray in the space following the surface, and the ray angle in both X-Z and Y-Z planes.

The PUPIL command is used to create a ray matrix file consisting of the number of rays specified in the command (i.e. PUPIL  $n$ ). If a WVL option is used followed by one or more wavelength numbers,  $n$  rays are traced at each wavelength. The total number of rays in the ray matrix cannot exceed 1000. The rays that comprise the ray matrix all start at the on-axis object point and proceed to the first surface (or the surface specified as the reference surface) where they form a uniformly distributed grid. The grid spacing is given by  $(A/n)^{.5}$  where  $A$  is the transmission

area and  $n$  is the number of rays. The transmission area is the area of the clear aperture minus any obstructions (Ref 2:83). Ray trace data are calculated and saved for subsequent calculations.

The ZPOLY command utilizes the ray matrix file generated by the PUPIL command and fits a set of Zernike polynomials to the optical path difference data contained in that file. The ZPOLY command calculates a geometrical approximation to the wavefront at the exit pupil. From this approximation, the Strehl ratio (discussed in Appendix III) is then calculated. A typical output from the ZPOLY command is shown in Figure 2-9.

#### Graphics Commands

The FALCON code has, within its repertoire, an extensive capability to generate graphic outputs. These commands yield the capability to generate system diagrams, energy distribution plots, wavefront maps, wave fans and spot diagrams. Each command is discussed individually with some of the more useful options. For a complete description of commands and options, refer to the FALCON User's Manual (Ref 2).

In order to produce graphic output, first the terminal must be prepared to accept graphic output from the Cyber computer. Procedures for doing this using the Tektronix 4025 terminal can be found in Appendix II. Secondly, the FALCON code must be placed in graphics mode by entering the command SYSTEM TEK ON. Without this command FALCON is

FIELD ANGLE 0.00 DEG

	TERMS	RMS
	0	.533
TILT	1	.533
FOCUS	2	.099
4TH ORDER	5	.054
6TH ORDER	9	.001
8TH ORDER	14	.000
10TH ORDER	21	.000

STREHL RATIO .678 AT DIFFRACTION FOCUS

FOURTH ORDER ABERRATIONS

MAGNITUDE	ANGLE	DESIGNATION
.285	90.0	TILT
4.380		DEFOCUS
.338	0.0	ASTIGMATISM
.261	90.0	COMA
.030		SPHERICAL ABERRATION

RADIAL COEFFICIENTS

ORDER	ZERNIKE	ASPHERIC	RAYS
2	2.185	4.363	.008726
4	.001	.006	.000024
6	.000	.000	.000000
8	.000	.000	.000001
10	.000	.000	.000001
12	.000	.000	.000000

Figure 2-9. ZPOLY Command Output.

capable of "line printer graphics" only.

The DISPLA command produces a cross sectional drawing of the optical system currently in active memory. This output provides a direct visual check on the construction of the system. Errors made in specifying the system resulting in incorrect curvatures, placement, or orientation can be immediately detected where numeric output would require close scrutiny to detect a similar mistake. By default, the optical layouts produced using the DISPLA command are drawn in the Y-Z plane. By including the option XZ after the DISPLA command the diagram is drawn in the X-Z plane. The optical layout is automatically scaled by FALCON, however, by including the option SCL sf, the scale factor, sf, may be specified by the user. The scale factor is displayed in the lower left corner of the output.

The LAYOUT command, alone or with the options described for the DISPLA command, produces output identical to that produced by the DISPLA command. The LAYOUT command differs from the DISPLA command in that it allows the user to draw rays on the diagram as well as optical surfaces. This is done by including the command, RAY f, on the LAYOUT command line or alone on subsequent command lines. The parameter f specifies the fractional distance within the reference surface at which the ray is drawn, hence the commands RAY 1 and RAY -1 would draw the marginal rays. An output using the LAYOUT command is shown in Figure 2-10.

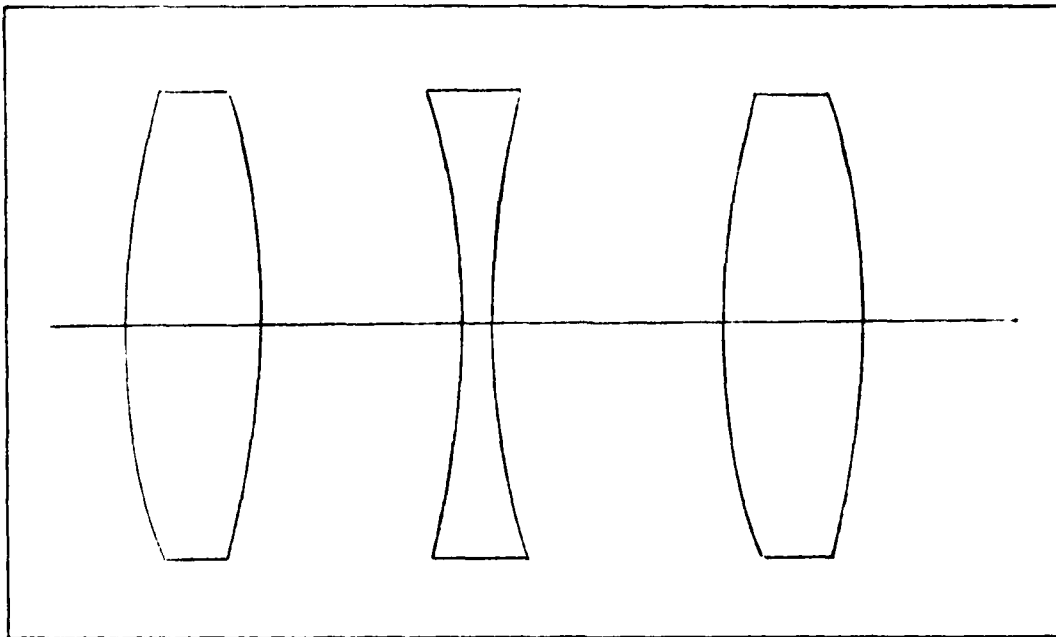


Figure 2-10. LAYOUT Command Output

There are two commands within FALCON that produce energy distribution plots (percent energy vs distance). The SPOT RED command calculates the fraction of rays that fall within a circle of given radius and displays the results as a function of radial distance (Ref 2:92). The output is called the radial energy distribution. It corresponds physically to the amount of energy transmitted through a variable aperture in the image plane. For afocal systems the radius is expressed in angular measure and the percentage of energy is expressed as a function of angular deviation.

There are several options available for use with the SPOT RED command. The CENT y x option allows the user

to specify the center of the energy distribution where  $y$  and  $x$  are specified in the image plane. Without the CENT option, FALCON calculates the centroid of the image and uses that point as the center of the energy distribution. The SCL  $r_{max}$   $i$  option allows the user to specify the maximum radius to be specified on the horizontal axis,  $r_{max}$ , and the increment used in plotting,  $i$ .

The ESCAN  $e$  option interpolates percent energy values from the data plotted and prints a table of these data in equal energy increments as specified by the parameter  $e$ .

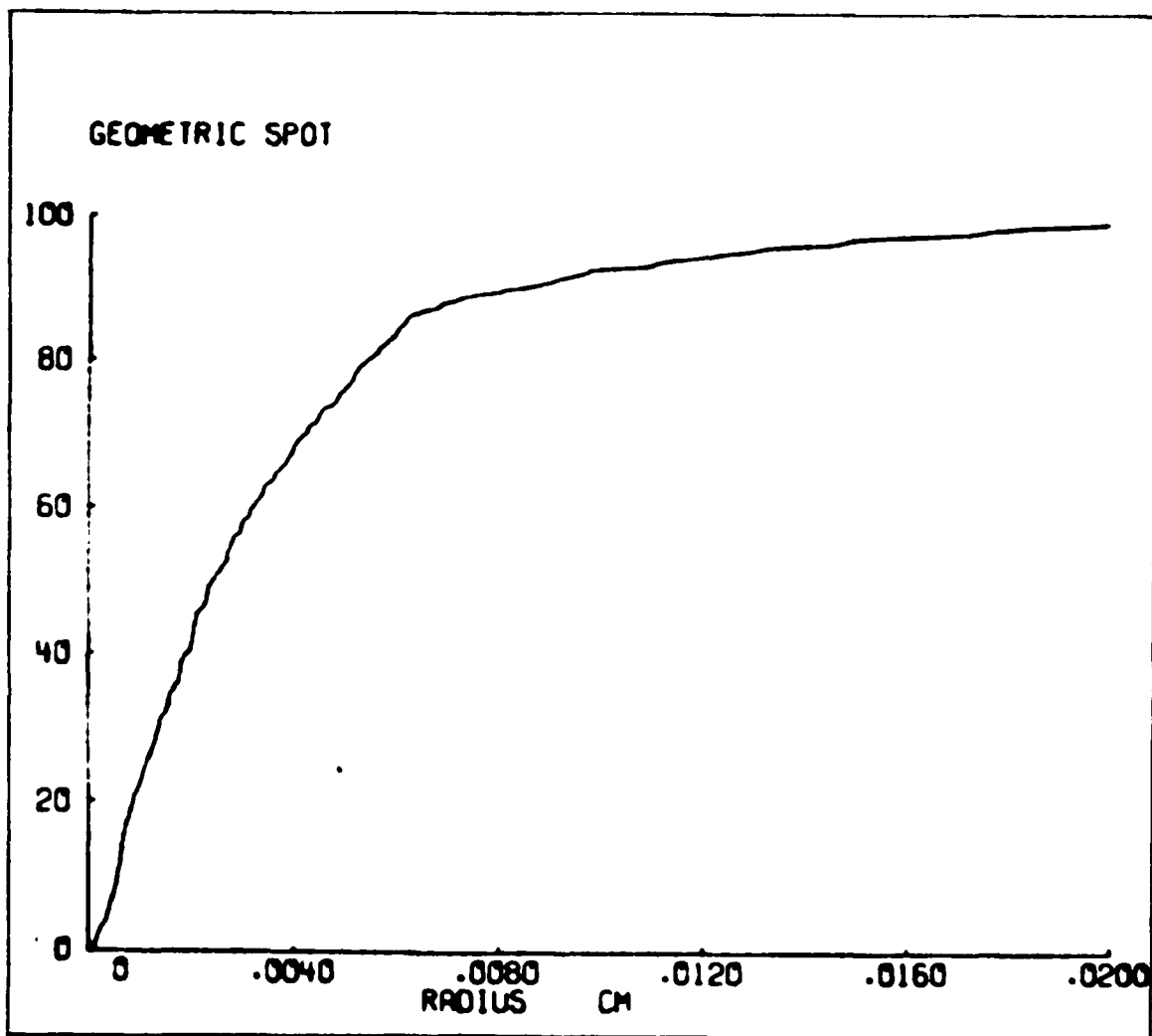


Figure 2-11. Radial Energy Distribution Plot

If no value for  $e$  is provided, the program defaults to an energy increment of five percent. Conversely, the LIST option prints out a table of percent energy values in equal increments of radius. The maximum radius and the increment are provided by the SCL option. A typical SPOT RED command output is shown in Figure 2-11.

The SPOT RED  $\theta$  command calculates and plots the fraction of rays that are uncovered as a straight knife is moved across the image plane. The parameter  $\theta$  is the

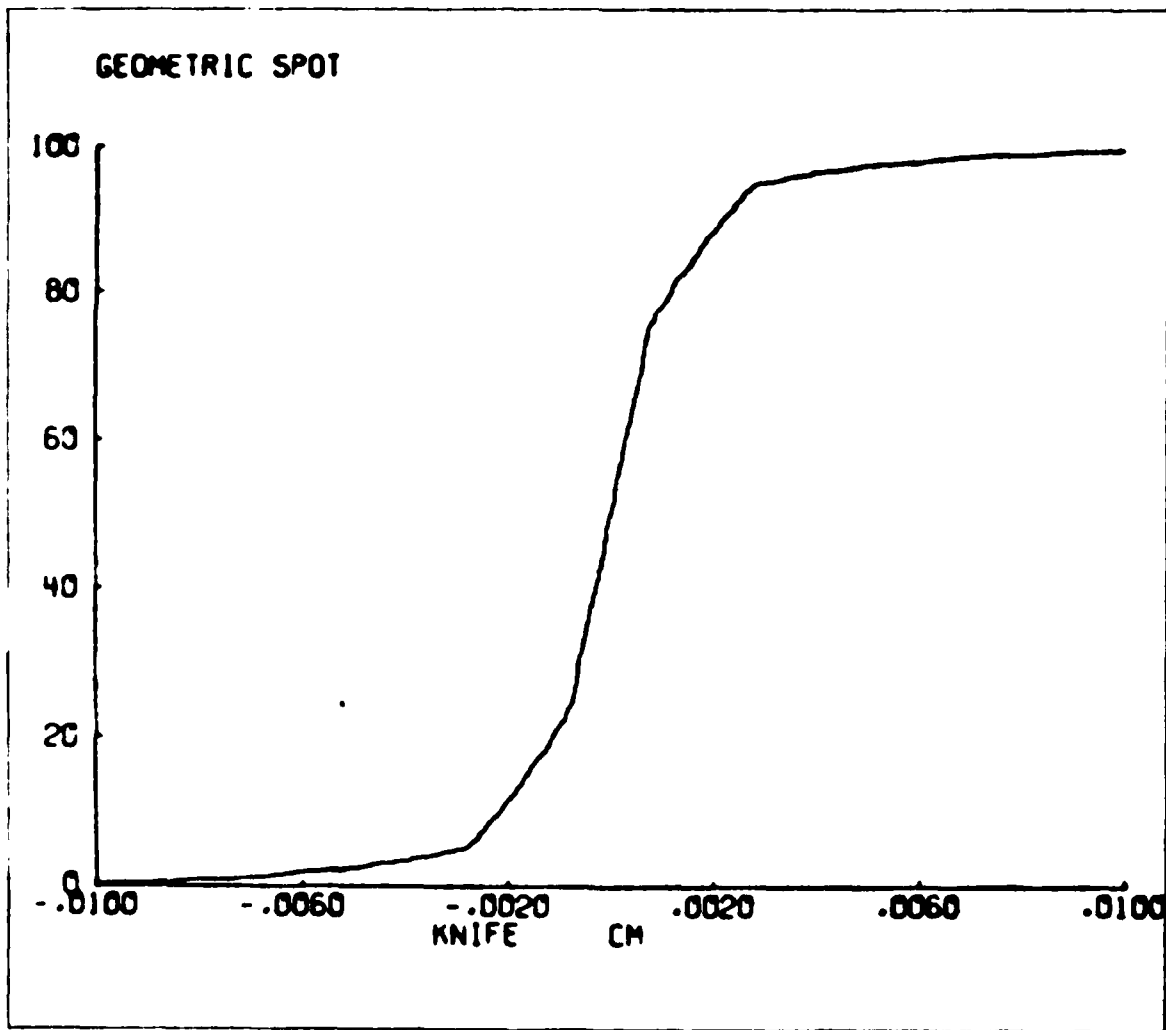


Figure 2-12. Knife Edge Distribution Plot

angle made by the knife edge and the Y axis. Positive angles result from clockwise rotations of the knife edge when looking from object to image in the positive Z direction (see figure 2-1). When  $\theta$  is zero, the knife edge is transparent to the left (positive X direction) and opaque to the right (negative X direction). The knife edge moves in a direction perpendicular to the edge so as to increase the unobscured aperture. If left unspecified, the program chooses a default value of zero for  $\theta$ . For the case where  $\theta$  equals zero, this corresponds to motion in the negative X direction. All options except CENT used with the SPOT RED command can be used with the SPOT KED command. A typical SPOT KED command output is shown in Figure 2-12.

The command WAMAP s generates a two dimensional contour plot of the wavefront at the image plane. The parameter s specifies the contour interval in wavelengths. If no contour interval is chosen, the program defaults to a value that will produce an uncluttered output. The wavefront is approximated by fitting a set of Zernike polynomials to the data in the ray matrix file generated by the PUPIL command, hence a PUPIL command must precede a WAMAP command. The WAMAP command generates a two dimensional contour plot of the wavefront as approximated by the set of Zernike polynomials. The PLOT3D s option causes the program to generate a three dimensional isometric plot of the wavefront. For this option the parameter s is a scale factor whose value must lie within the interval  $0 \leq s < 1$ . Typical WAMAP and WAMAP PLOT 3D outputs

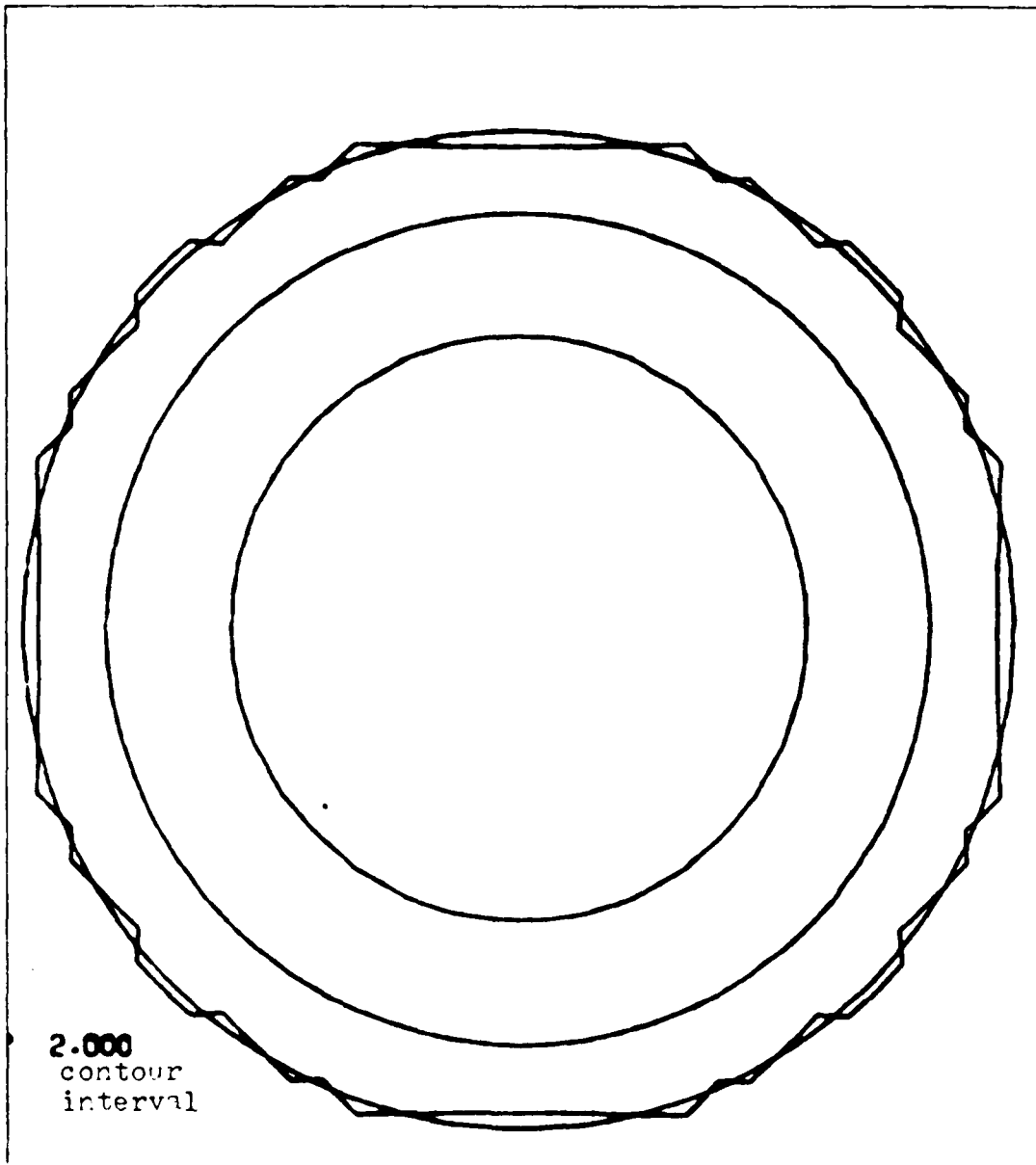


Figure 2-13. Contour Wavefront Plot

are shown in Figures 2-13 and 2-14, respectively.

A fan of rays is a collection of rays that starts from the same object point and intersects the reference surface (i.e. the first surface unless otherwise specified) at equally spaced distances along a specified line (Ref 2:75). The FANS v command generates two sets of fans for each

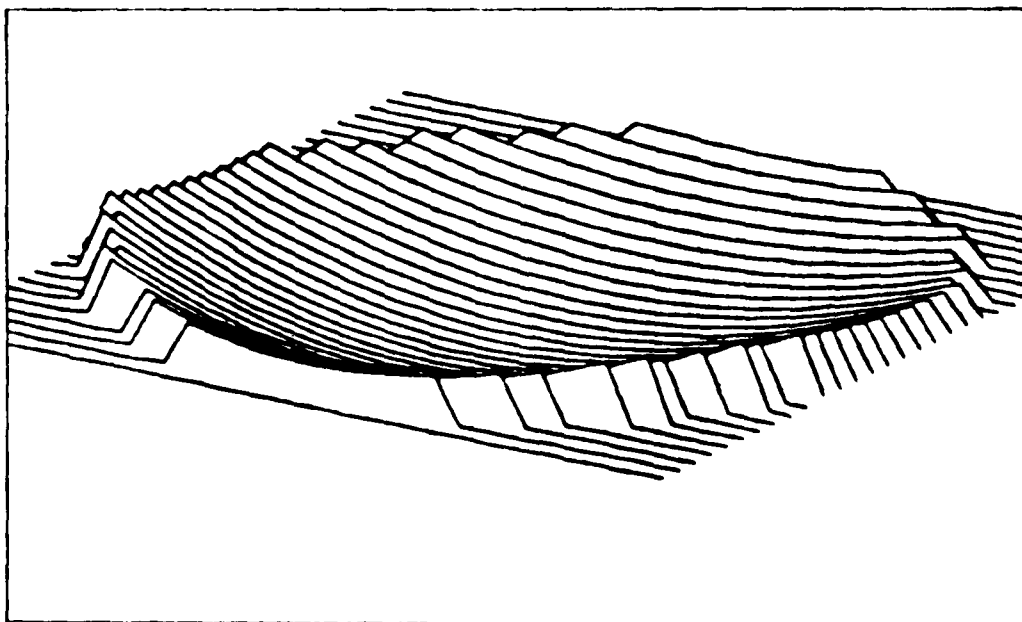


Figure 2-14. Isometric Wavefront Plot

off-axis object point. One fan is traced in the tangential plane (the Y-Z plane). The line of intersection for this fan with the reference surface is the Y axis. The other fan, traced in the sagittal plane, intersects the reference surface along the X axis (Ref 2-75). These rays are called skew rays. Skew rays have both X and Y components, however, only the Y component is displayed. Only the tangential plane is displayed at zero to avoid duplicating information. The sagittal fan plot is an odd function (symmetric about the origin) so only the results for the positive X axis is plotted. The optional parameter,  $v$ , allows the user to specify the vertical scale. The FOBS  $f_1 f_2 f_3$  option allows the user to select three fractional field positions for the object point. If this option is not used, the default value for  $f_1$ ,  $f_2$ , and  $f_3$  are 1, .707, and 0 respectively. The WVL

option allows the choice of up to three previously specified wavelengths. This is done by including on the FANS command line, the identifier WVL followed by the desired wavelength numbers (one through five). A typical FANS command output is shown in Figure 2-15.

The tangential and sagittal fans previously discussed take into account only those rays passing through a cross shaped aperture over the reference surface. To include all possible skew rays it is necessary to divide the lens aperture into a uniform grid, place a ray intersection at each grid intersection, and trace these rays through the optical system. By assuming that each ray carries the same amount of energy, the intersection of these rays with the Gaussian focal plane will be a fair representation of the image that can be expected (Ref 11:152).

The SPOT PLOT command generates such a grid of rays on the reference surface, the rays for which all start at the on-axis object point. The number of rays is specified by the PUPIL command and previously stored in the ray matrix file. By using the SPOT PLOT command, up to 1000 rays can be traced through the system to the image plane. The resulting spot diagram is a graphic representation of the intersection of these rays with the image plane.

There are several options that can be used with the SPOT PLOT command. The SPOT v option specifies the scale of the plot. By specifying a value for the parameter v, the user can control the overall size of the diagram. Larger numbers

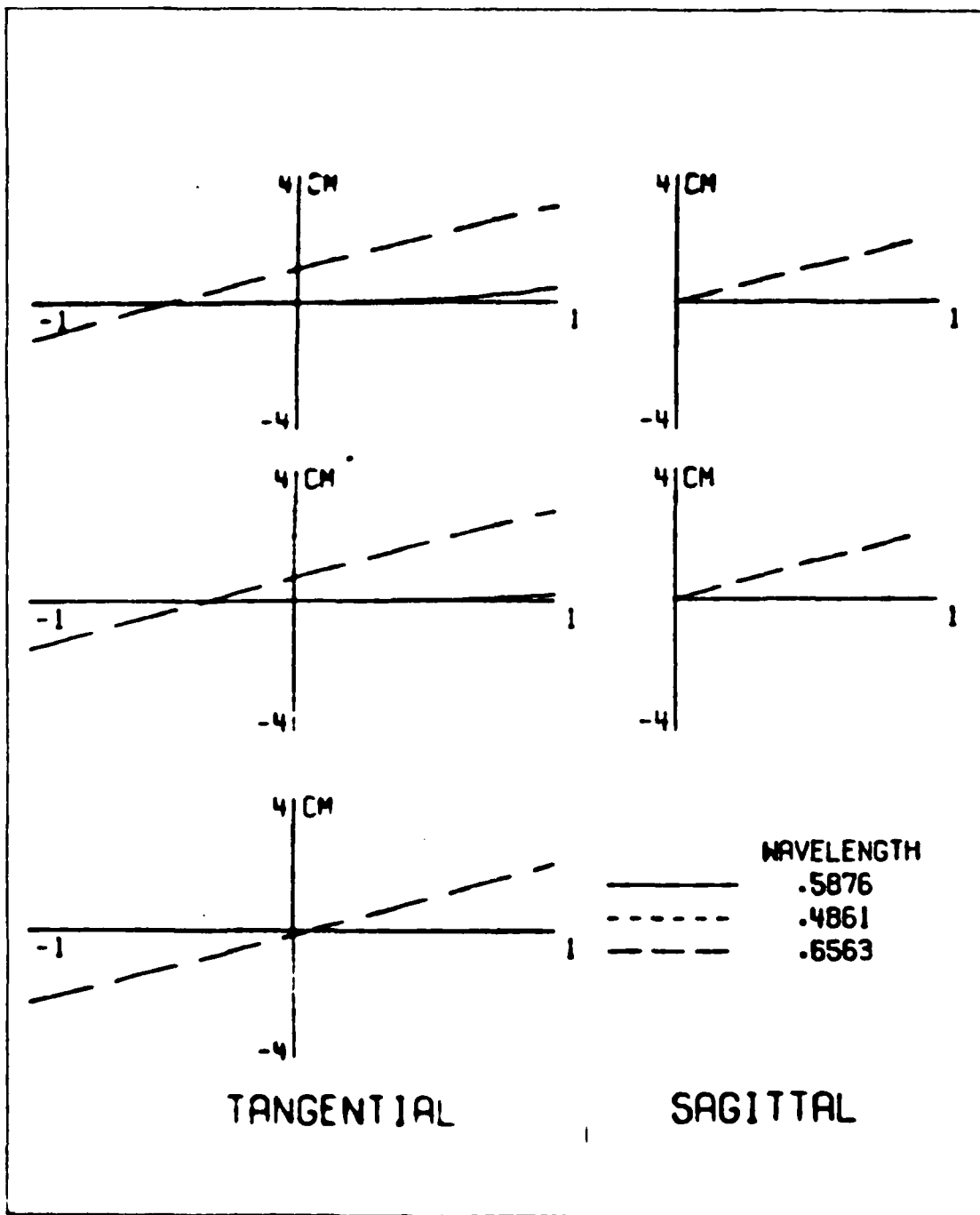


Figure 2-15. Fan Plots

for  $v$  yield smaller plots and vice versa. The OFFSET  $x_c$   $y_c$  option allows the user to shift the position of the spot diagram on the screen or page. The shift in origin occurs at the image plane. The PUPIL option calculates the shift necessary to transfer the spot diagram from the image plane to the exit pupil plane. The SYMBOL option causes the use of a different plotting symbol (in lieu of dots) for each

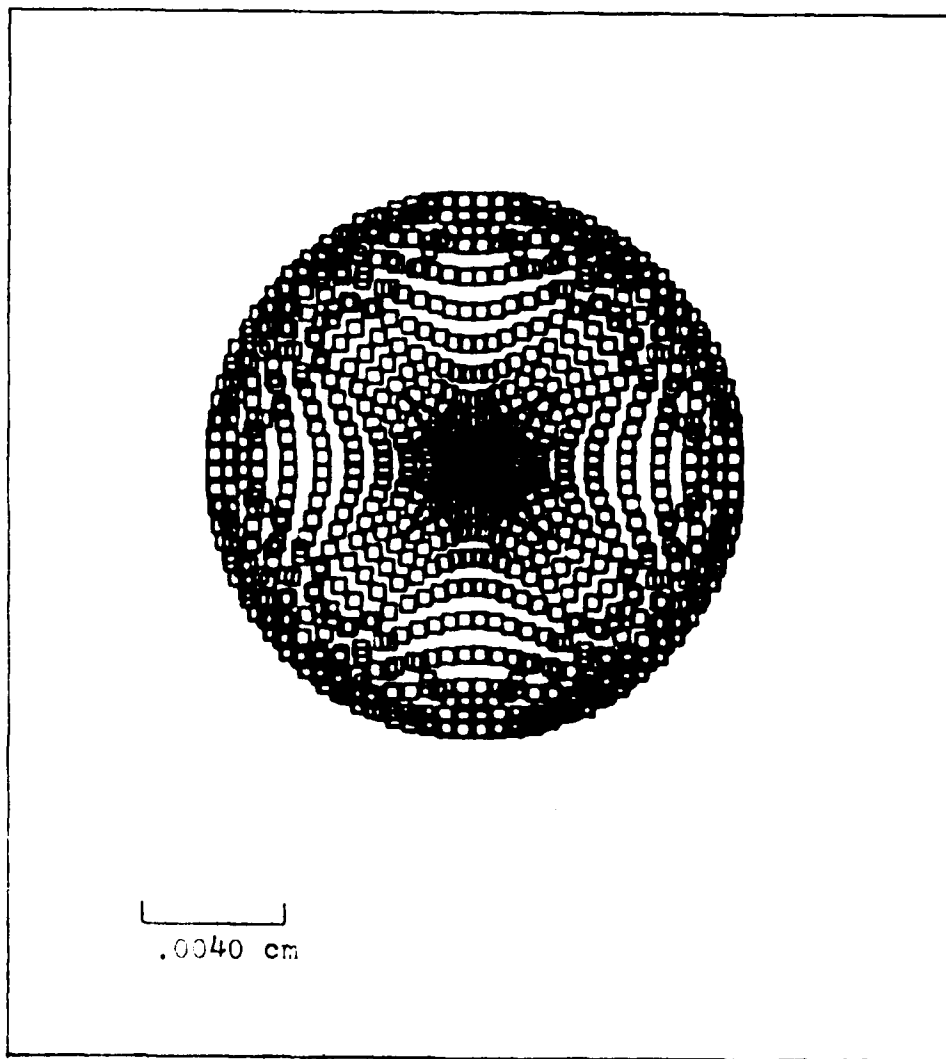


Figure 2-16. Spot Plot

wavelength being traced. This aids in isolating color effects. A sample SPOT PLOT IS shown in Figure 2-16.

## Lens Library

The FALCON program has the provision to store many optical systems in permanent storage in library files. These files are maintained by the FALCON program. Individual data sets may be inserted, retrieved, and deleted. The command governing all library functions is LIB. The options PUT, GET, DEL, and CAT instruct the program to insert, retrieve, delete, and comprehensively list data sets (lens decks) by name. After the PUT, GET, or DEL option is specified, a data set name must be included. If using the PUT option a new name of the user's choosing is specified. To retrieve or delete a data set the user must specify a previously stored data set name. The CAT option lists each data set in the library by the name assigned to it.

### III. TRIPLET EVALUATION

In this chapter the use of the FALCON code is demonstrated by evaluating a particular type of lens known as a Cooke triplet. The Cooke triplet consists of a single negative lens between two positive lenses, separated by air spaces (Ref 3:10-1). This lens is used for demonstration because it illustrates most of the problems encountered in the design of any optical system. Many other types of lenses are either composed of or derivatives of the basic triplet design (e.g. TESSAR, SONNAR, and MAGNAR telephoto) (Ref 4:238) (Ref 15:160). The triplet is used extensively as a photographic objective (Ref 3:10-1).

The Cooke triplet was originally designed by H. D. Taylor in 1895 who described how he was able to correct astigmatism and field curvature using three lens elements separated by air spaces (Ref 3:10-1). Full advantage was taken of the various parameters which can be altered in a system of three separated elements (Ref 4:238). Figure 3-1 shows the triplet to be evaluated.

Using the method described by Lea, (Ref 5:42) the triplet was first evaluated using manually performed paraxial raytrace calculations. These calculations were then used to verify the output of FALCON.

The triplet was examined in three slightly different configurations to observe the changes resulting from adjusting the distance between surfaces 4 and 5, and from an off axis object point. The triplet chosen is taken from the

Triplet Description. The triplet is composed of three transmissive elements aligned on a common axis, each having two spherical surfaces. All distances within the system are measured on the optical axis. In the original triplet system as published, the object surface is located 25 cm to the left of the first surface. The axial ray strikes the first surface at a height of 1.25 cm above the optical axis. The first surface has a radius of curvature of 3.9549 cm. The glass from which the first element is constructed has an index of refraction of 1.620. The thickness of the first element is 0.6 cm. The second surface has a radius of curvature of -68.02 cm. By convention, spherical surfaces whose concave surfaces lie to the right have positive radii of curvature. There is an air space between surfaces two and three whose thickness is 0.15 cm. Surface three, following the air space, has a radius of curvature of -5.015 cm followed by a 0.15 cm thickness of glass with a refractive index of 1.621. Surface 4, comprising the right hand side of element 2, has a radius of curvature of 3.850 cm. An air space of 1.13691 cm follows element 2. The air space is followed by surface 5 having a radius of curvature of 19.743 cm. Element 3 has a thickness of 0.6 cm and is constructed of glass with a refractive index of 1.620 as is element 1. Element 3 is followed by an air space. The lens arrangement is shown schematically in Figure 3-1 with some of the notation used in this chapter.

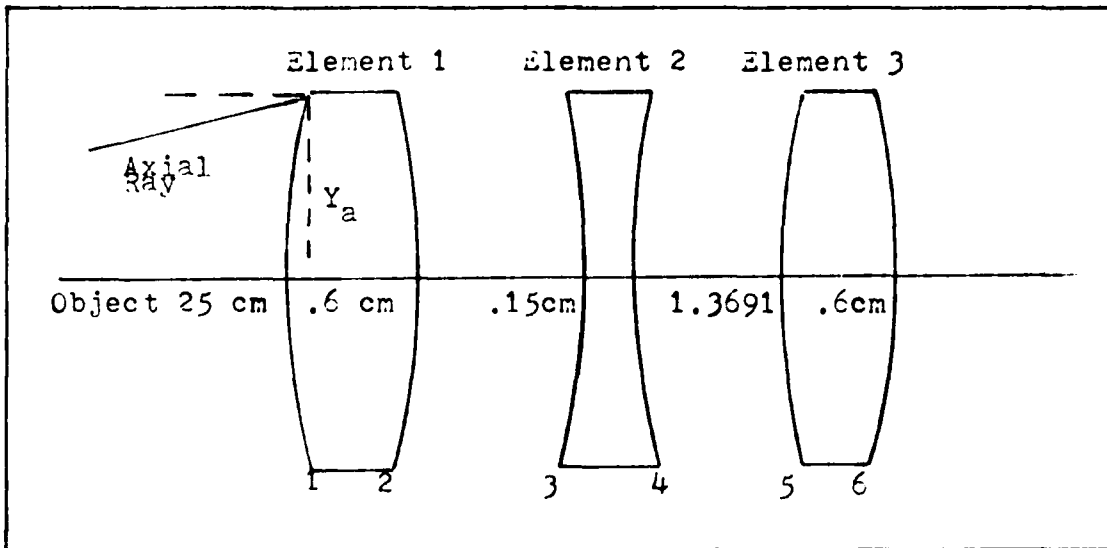


Figure 3-1. Cooke Triplet

### Manual Ray Tracing

In order to gain confidence in the outputs of the FALCON code, a manual paraxial ray trace was performed. The results were compared with some of the code's output with good agreement (to be discussed in some detail later). The manual calculations also serve to demonstrate some of the internal workings of the code. Ray tracing will be performed using the method described by Lea (Ref 5) and is demonstrated in the paragraphs that follow.

To begin, each known parameter is entered into the first section of the ray trace table as in Figure 3-2.

Surface	1	2	3	4	5	6	7	8
Curvature	0.0	.25285	-.01474	-.19942	.25973	.05065	-.24588	0.
Thickness	25.0	0.6	1.06541	0.15	1.13691	0.6	14.050	
Index	1.00	1.620	1.00	1.621	1.00	1.620	1.00	

Figure 3-2. Ray Trace Table (First Section)

For purposes of these calculations, thickness (t) is measured in centimeters, curvature (c) is defined as the reciprocal of the radius of curvature (in cm), and the index refraction (n) is dimensionless.

The second section of the ray trace table can now be completed using calculated values of the "reduced thickness" (t/n) and the power P ( $P = \{n' - n\}c$ ). The variable n' represents the index of refraction of the medium following the surface currently under consideration. The completed second section of the ray trace table is shown in Figure 3-3.

Surface	1	2	3	4	5	6	7	8
Power	-.15677	-.00914	.12384	.16229	-.03140	-.15245		
t/n	25.0	.37037	1.06541	.09254	1.13691	.37037	14.0515	

Figure 3-3. Ray Trace (Second Section)

Once the second section is completed, the first section is no longer needed. At this point, all known information is inserted into the third and final section of the ray trace table. In this section of the table, y represents the height of a ray above the optical axis measured at a surface. The variable u represents the angle, measured with respect to the optical axis, at which a ray enters or leaves a given surface. The subscript "a" denotes the axial ray (starting from the on-axis object point) and the subscript "b" denotes the chief ray (passing through the center of the aperture stop). Using what Lea describes as the "mindless hop, skip and jump approach", the refraction equation (3.1) and the transfer equation (3.2) yield values

to complete section three of the ray trace table. The completed third section is shown in Figure 3-4.

Surface	1	2	3	4	5	6	7	8
$Y_a$	0.0	1.25	1.19594	1.02879	1.02606	1.18070	1.21743	0.0
$nu_a$	.050	-.14596	-.15689	-.02948	.13601	.09894	-.08664	
$Y_b$	-10.0	-.75	-.56942	-.04440	.00069	.55481	.72887	5.7738
$nu_b$	.37	.48758	.49278	.48728	.48739	.46997	.35886	

Figure 3-4. Ray Trace Table (Third Section)

This method has the distinct advantage that several other system parameters can readily be calculated from the information contained in the ray trace table. From an examination of the axial ray trace data (subscripted "a"), the following parameters are easily calculated.

1. Back Focal Length (bfl)

$$bfl = -y_{a7}/u_{a8} = 1.21734/-.08664 = -14.051$$

2. Effective Focal Length (efl)

$$efl = -y_{a2}/u_{a8} = -1.25/-.08664 = 14.42$$

3. Numerical Aperture (NA)

$$NA = n_8 \sin u_{a8} = \sin .08664 = .08653 \text{ (rad)}$$

4. Lateral Magnification ( $M_1$ )

$$M_1 = u_{a2}/u_{a8} = -.057$$

5. F=Number (F#)

$$f\# = 1/[2(NA)] = 1/[2(.08653)] = 5.778$$

By inspection of the calculated ray trace values for the principal ray (subscripted "b"), the following parameters are available.

1. Field Angle  $u_{b2} = 20.63$  degrees

2. Image Height  $y_{b8} = 17.63$  cm

From a single calculation, the Lagrange invariant can also be calculated by the relation

$$H = n(u_a y_b - u_b y_a).$$

The Lagrange invariant,  $H$ , can be evaluated at any point in the system for which the above paraxial ray trace parameters are known. The value of  $H$  should remain constant throughout the system. The square of the Lagrange invariant is a measure of the information capacity of a system (i.e. how many independent points can be resolved by the system. For the hypothetical optical system without aberrations, the system is said to be diffraction limited; that is to say the spot size is limited by diffraction in the aperture of the system (Ref 5:50). For the diffraction limited case, the number of resolvable spots,  $N$ , is given by the equation

$$N = 4H^2/\lambda^2$$

where  $\lambda$  is the wavelength being considered. The value of  $H$  is a direct measure of the difficulty of design and manufacture (Ref 5:51).

### Achromatic Aberrations

In discussions of aberrations it is convenient to define two planes as follows: The tangential plane, from which the angle  $\theta$  is measured, is the plane containing the optical axis and the off axis object point; throughout the system the chief ray lies in the tangential plane (see Figure 3-5). The sagittal plane is that plane which contains the chief ray and is perpendicular to the tangential plane throughout the system. There is only one tangential plane throughout the system whereas the sagittal plane changes as one proceeds to different spaces throughout the system (Ref 6:308).

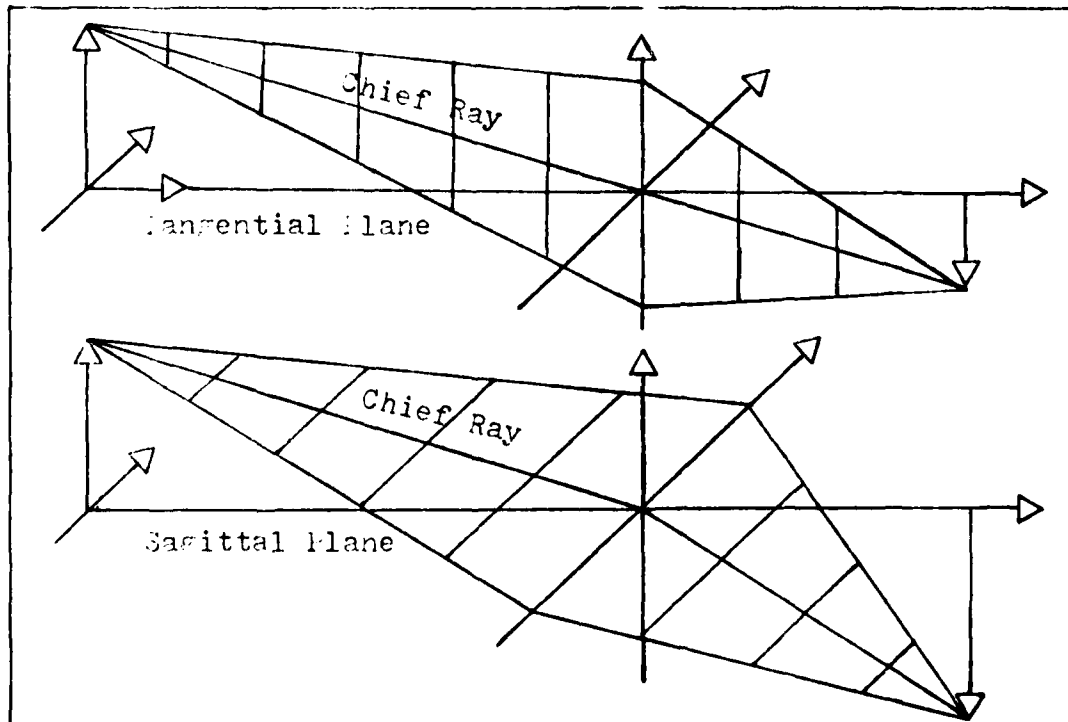


Figure 3-5. Tangential and Sagittal Planes (Ref 5:82)

The tangential and sagittal planes are simply vertical and horizontal sections of the imaging bundle (Ref 5:82). As the central ray of the imaging bundle, the principal ray is the only ray that lies in both the tangential and sagittal planes.

Wavefront Aberration Function. Any given wavefront can be represented by a function of the three variables  $r'$ ,  $h'$ , and  $\theta$  as shown in Figure 3-6. If the wavefront,  $W$ , exiting an optical system is expanded in terms of these three variables, and if those terms allowed by symmetry arguments are discarded, the resulting polynomial can be written as

$$\begin{aligned}
 W = & a_1 r'^2 + a_2 h' r' \cos \theta + \pi_1 r'^4 \\
 & + \pi_2 r'^3 h' \cos \theta \\
 & + \pi_3 r'^2 h'^2 \cos^2 \theta \\
 & + \pi_4 r'^2 h'^2 \\
 & + \pi_5 r' h'^3 \cos \theta \\
 & + \text{Higher Order Terms.}
 \end{aligned}$$

Ignoring the higher order terms, the coefficients  $a_1$  and  $a_2$  are identified as defocus and sideways shift, respectively. The coefficients  $\pi_1$  through  $\pi_5$  are identified as spherical aberration, coma, astigmatism, field curvature, and distortion, respectively.

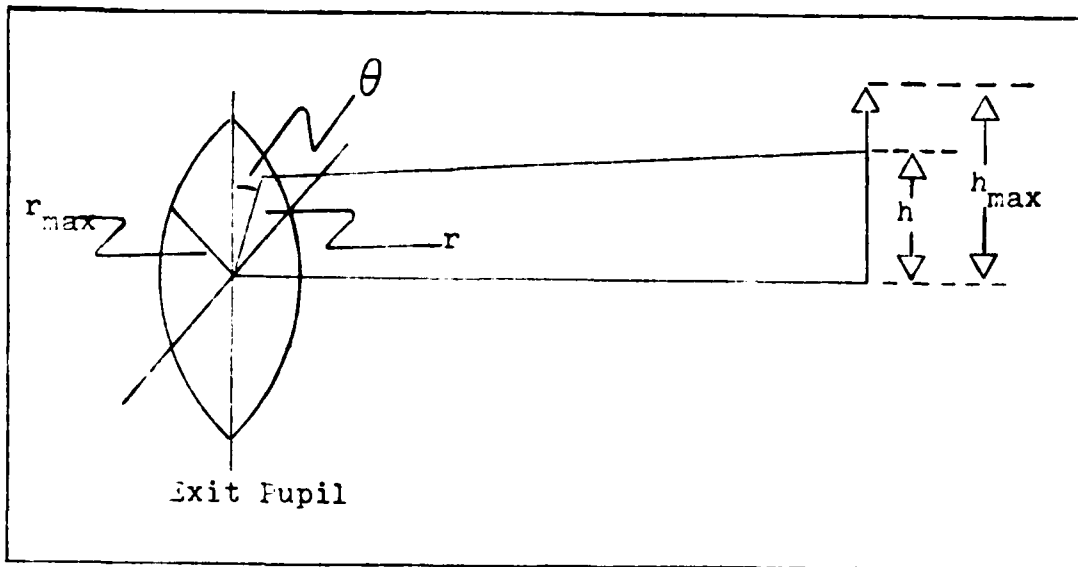


Figure 3-6. Wavefront Aberration Function Parameters

A coarse measure of the quality of the image produced by an optical system is Optical Path Difference (OPD). The OPD is the deviation of the real wavefront from an ideal, perfectly spherical reference wavefront at full aperture and field.

The OPD is simply a linear measure often expressed in terms of the wavelength under consideration. A root mean square OPD of one quarter of a wavelength indicates an essentially diffraction limited system (Ref 5:88). According to Rayleigh, there is no appreciable deterioration of the image if the phase difference does not exceed  $\pi/2$  (Ref 6:287). Thus, the image quality of the wavefront will not be seriously impaired provided the wavefront aberration does not exceed one quarter of a wavelength. It is often the case where individual wavefront aberration coefficients are

quoted as OPD's. By setting the values of  $r'$  and  $h'$  both equal to 1, where  $r'=r/r_{\max}$  and  $h'=h/h_{\max}$ , in the wavefront polynomial, the coefficients  $\pi$  are OPD's (Ref 5:88).

Seidel Aberration Function. In an aberrated optical system, each ray will miss its Gaussian image point by an amount  $(\epsilon_x, \epsilon_y)$ . The quantities  $\epsilon_x$  and  $\epsilon_y$  can each be expanded in a power series in  $r'$ ,  $\theta$ , and  $h'$  as follows:

$$\begin{aligned}\epsilon_x &= \sigma_1 r'^3 \sin \theta + \sigma_2 r'^2 h' \sin 2\theta \\ &\quad + (\sigma_3 + \sigma_4) r' h'^2 \sin \theta \\ \epsilon_y &= \sigma_1 r'^3 \cos \theta + \sigma_2 h' (2 + \cos 2\theta) \\ &\quad + (3\sigma_3 + \sigma_4) r' h'^2 \cos \theta \\ &\quad + \sigma_5 h'^3\end{aligned}$$

The coefficients  $\sigma_1$  through  $\sigma_5$  are the third order or Seidel coefficients. The Seidel coefficients relate to the wavefront coefficients (the  $\pi$ 's) by the following relations:

$\sigma_1 = 4 \pi_1 / n_k u_{ak}$	Spherical aberration
$\sigma_2 = \pi_2 / n_k u_{ak}$	Coma
$\sigma_3 = \pi_3 / n_k u_{ak}$	Astigmatism
$\sigma_4 = (2\pi_4 - \pi_3) / n_k u_{ak}$	Field Curvature
$\sigma_5 = \pi_5 / n_k u_{ak}$	Distortion

The third order Seidel coefficients are used extensively in optical design; the aim of the exercise being to drive them all to zero. This is usually impossible, however, and the art of lens design is in deciding what balance of aberrations will give best results.

Third order Seidel coefficients can be directly calculated entirely from paraxial ray trace data as was generated earlier (pages 35-37) (Ref 5:92). The applicable equations are given in Figure 3-7.

$$\begin{aligned} \sigma_1 &= -1/(2n'_k u'_{ak}) \Sigma S_a i_a^2 \\ \sigma_2 &= -1/(2n'_k u'_{ak}) \Sigma S_a i_a i_b \\ \sigma_3 &= -1/(2n'_k u'_k u'_{ak}) \Sigma S_a i_b^2 \\ \sigma_4 &= -1/(2n'_k u'_{ak}) \Sigma c/n' (n/n'-1)H^2 \\ \sigma_5 &= -1/(2n'_k u'_{ak}) \Sigma [S_b i_a i_b \\ &\quad - H(u'_b{}^2 - u_b{}^2) \\ S_a &= n(n/n' - 1)y_a (i_a + u'_a) \\ S_b &= n(n/n' - 1)y_b (i_b + u'_b) \\ i &= yc + u \end{aligned}$$

Figure 3-7. Seidel Coefficients (Ref 5:93)

Calculating the Seidel coefficients is simply a matter of substituting the appropriate quantities from the paraxial ray trace table into the equations of Figure 3-7 and performing the necessary algebra.

#### Triplet Analysis Using FALCON Code

The FALCON code is capable of performing most functions involved in the analysis and design of optical systems. For the purpose of analyzing a given design, many of these capabilities will be exercised. Start-up procedures for running the FALCON code are described in detail in Appendix II.

System Input. Once FALCON is operating interactively, the LENS statement is used to place the program into the mode where it can accept specifications for a given optical system.

Special entries are available to specify the starting conditions of the axial and chief rays. The next several lines, in general, will specify surface profiles, distances between surfaces, and indices of refraction. The Cooke triplet being considered here uses only spherical surfaces, requiring the input of only a radius of curvature or its reciprocal (i.e. the curvature) to specify the surface profile. Although the FALCON program is capable of dealing with conics and higher order aspherics, it is not necessary to utilize these capabilities for the triplet.

The lens specification for the Cooke triplet being considered is shown in Figure 3-8.

```
LENS (1)
LI COOKE TRIPLET EXAMPLE (2)
SCY - 10 SAY 1.25 TH 25 UNITS CM (3)
CV .25285 TH .6 GLASS 1.62 (4)
CV -.01474 TH 1.06541 GLASS 1.0 (5)
CV -.199420 TH .15 GLASS 1.621 (6)
CV .25973 TH 1.13691 GLASS 1.0 (7)
CV .05065 TH .6 GLASS 1.62 (8)
CV -.24588 TH 14.05015 GLASS 1.0 (9)
END
```

Figure 3-8. FALCON Lens Specification - Cooke Triplet

Line (1) is the LENS command line placing the FALCON code in the mode where it is capable of accepting specifications for an optical system. Line (2) is the caption/identifier line. Line (3) contains the SAY identifier, which defines the height at which the axial ray strikes the first surface, and the SCY identifier which defines the height on the object at which the chief ray begins. In line (3) the thickness identifier, TH, defines the distance between the object and the first surface. In lines (4), (5), (6), (7), (8), and (9), the CV identifier defines the curvature of the respective surface. The TH identifier defines the distance between the surface under consideration and the next surface in centimeters. The GLASS identifier defines the index of refraction of the medium following each surface. The last line, (10), contains only the word END which directs the program to return from lens specification mode. The numbers in parentheses following each line are included for reference only and are not part of the lens specification.

After specifying the optical system, FALCON is ready to begin with a host of analysis functions at the operators command. A comparison of the output resulting from the PARAX command with manual paraxial ray trace data lends credence to the accuracy of the FALCON code. All axial and chief ray heights agree to within five decimal places. The same agreement holds for axial and chief ray angles. This provides assurance that the system believed to have been entered does in fact reside in the FALCON library. The effective focal length, back focal length, and F-number

FIELD ANGLE 0.00 DEG

BI-LATERAL SYMMETRY INVOKED

	TERMS	RMS
	0	1.454
TILT	1	1.454
FOCUS	2	.192
4TH ORDER	5	.099
6TH ORDER	9	.007
8TH ORDER	14	.000
10TH ORDER	21	.000

STREHL RATIO .235 AT DIFFRACTION FOCUS

FOURTH ORDER ABERRATIONS

MAGNITUDE	ANGLE	DESIGNATION
.000	0.0	TILT
-9.990		DEFOCUS
.000	0.0	ASTIGMATISM
.000	0.0	COMA
-2.203		SPHERICAL ABERRATION

RADIAL COEFFICIENTS

ORDER	ZERNIKE	ASPHERIC	RAYS
2	-4.987	-4.987	-.009974
4	-.369	-8.480	-.033919
6	.262	2.978	.017867
8	.020	.851	.006805
10	.001	.140	.001404
12	.000	.049	.000593

Figure 3-9. ZPOLY LIST Output

resulting from the LEPRT command also exhibit similar agreement with manual calculations.

The ZPOLY LIST command produces several outputs as discussed in Chapter 2. Among these, the Strehl Ratio (discussed in Appendix IV.) was calculated to be 0.235 indicating a high loss in peak intensity due to aberrations. The ZPOLY LIST output is shown in Figure 3-9 for the triplet as published. The two dominant fourth order aberrations are defocus at  $-9.99$  wavelengths and spherical aberration at  $-2.203$  wavelengths. Since defocus does not enter into the calculation of the Strehl ratio, spherical aberration will be examined.

In the absence of all aberrations except spherical aberration, the aberration function  $W$  is proportional to the fourth power of the aperture radius. Those rays entering the paraxial region come to a focus at the Gaussian focus. Those rays entering in the marginal region intersect the optical axis at the marginal focus. Those rays entering the system in intermediate regions intersect the optical axis somewhere between the Gaussian focus and the marginal focus (Ref 6:309). One is then led to believe that by shifting the focus to somewhere between the marginal and Gaussian foci (e.g. circle of least confusion) that the spherical aberrations can be reduced. A shift in focus was accomplished by adjusting the distance between the second and third elements from 1.13691 cm to 1.07600 cm.

The result was as expected; the spherical aberration

decreased from -2.203 to -0.067 wavelengths. This resulted in an increase in the Strehl ratio from 0.235 to a somewhat more respectable 0.648. The adjustment did, however, increase the defocus from -9.999 to 12.384. The inclusion of an aperture to limit incoming rays to the near paraxial region should serve to reduce spherical aberration, however time constraints precluded further investigation. To reduce the defocus the distance from surface 6 to the image plane was increased from 14.05015 cm to 14.15522 cm. This reduced the defocus to 0.000 wavelengths. The image plane adjustment did slightly increase the magnitude of the spherical aberration from -0.067 wavelengths to -0.078 wavelengths. The Strehl ratio remained at 0.648.

The elements of the new system (Strehl ratio =0.648) were displaced from the optical axis a distance of -1.25 cm. The result was a system for which the effects of an off-axis object could be evaluated. Table 3-1 and 3-2 summarize the system parameters for the three systems being considered.

System Description	Distance Between Surfaces (cm)					
	1-2	2-3	3-4	4-5	5-6	6-7
Original Triplet	0.60	1.06541	0.1500	1.13691	0.600	14.05015
Adjusted Triplet	0.60	1.06541	0.1500	1.07600	0.600	14.15522
Decentered Triplet	0.60	1.06541	0.1500	1.07600	0.600	14.15522

Table 3-1 Triplet Intersurface Distances

System	Aberrations (in wavelenths at .58746 nm)					
<u>Description</u>	<u>Tilt</u>	<u>Defocus</u>	<u>Astig.</u>	<u>Coma</u>	<u>S.A.</u>	<u>S.R.</u>
Original	0.000	-9.999	0.000	0.000	-2.203	.235
Adjusted	0.000	0.000	0.000	0.000	0.078	.648
Decentered	2.547	1.331	1.374	1.768	-0.549	---

Table 3-2. Triplet Aberrations and Strehl Ratio

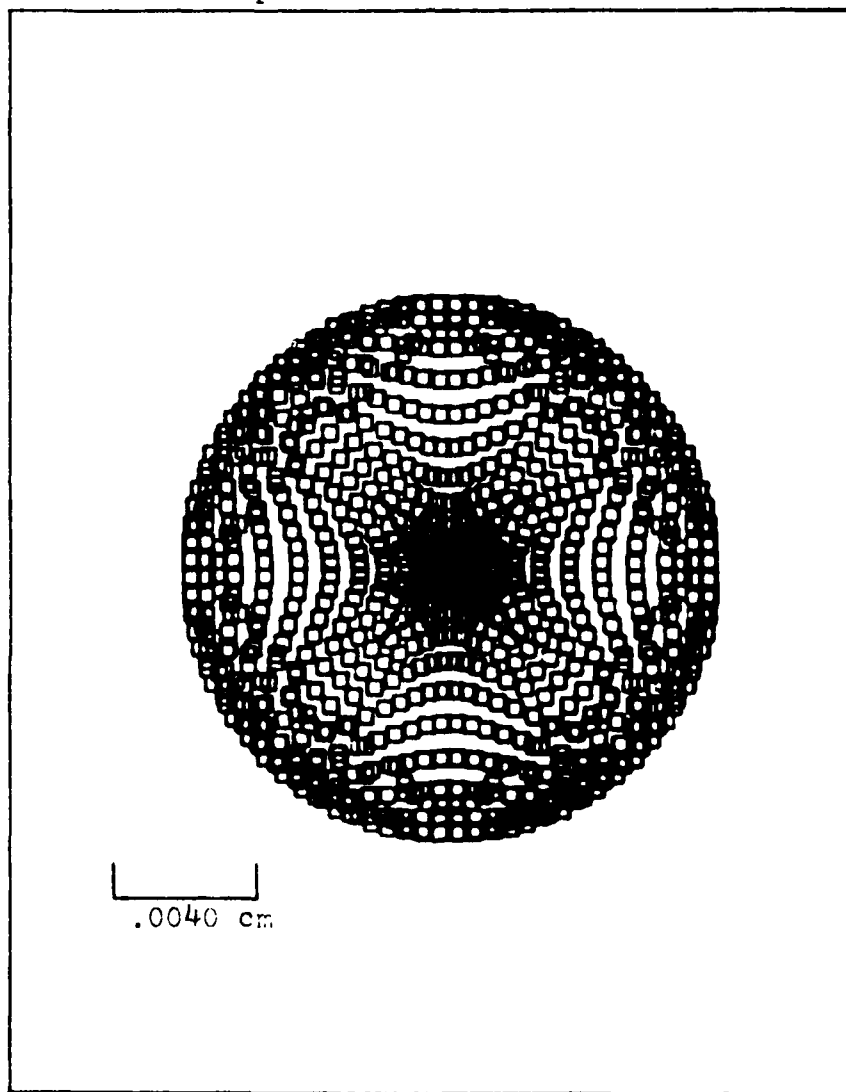


Figure 3-10. Spot Diagram for Original Triplet

A spot diagram for the original triplet is shown in Figure 3-10. The pattern shown represents a spot in the focal plans consisting of 950 rays with an overall diameter of 0.014 cm. The density of rays within the pattern is a measure of the intensity distribution in the focal plane.

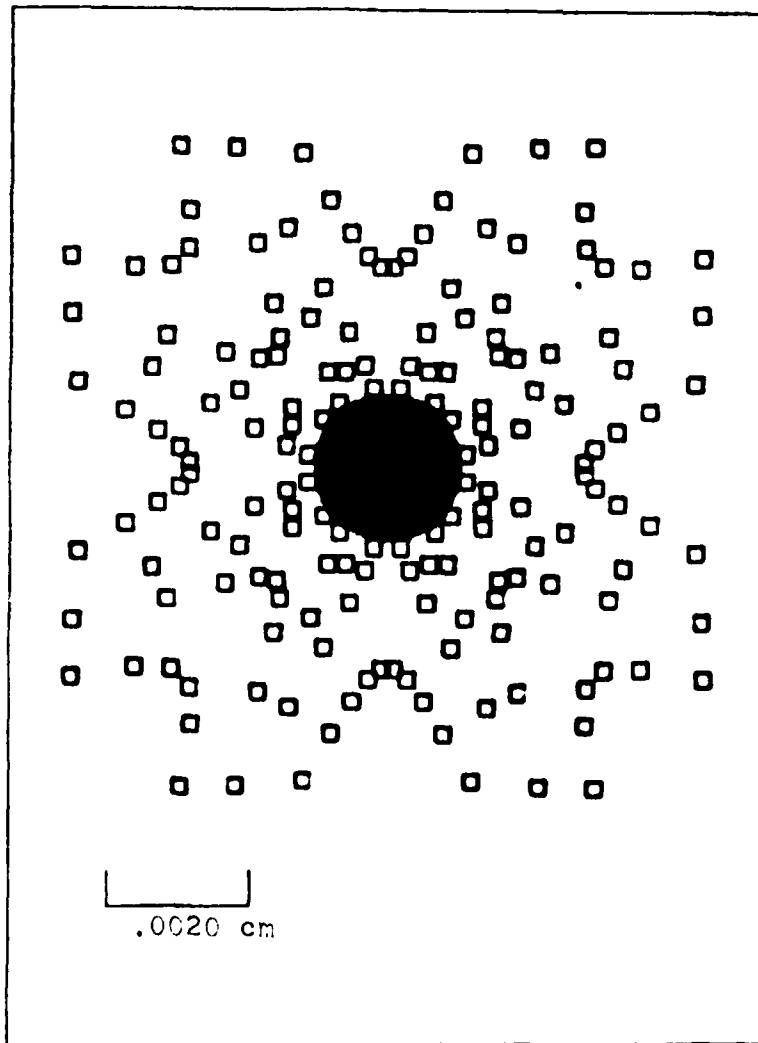


Figure 3-11. Spot Diagram for Adjusted Triplet

After the system was adjusted by decreasing the distance between elements two and three from 1.13691 cm to 1.07600 cm and by moving the focal plane to the position where the wave-

front defocus was reduced to 0.000 wavelengths, a spot diagram was again made. This spot diagram is shown in Figure 3-11. The vast majority of rays in this diagram are seen to cluster in a central bright spot. The diameter of the central spot in this case is approximately 0.0020 cm while the maximum diameter of the entire pattern is 0.0096 cm. As expected, with the lower aberrations in the case of Figure 3-11, a more tightly focused spot is possible.

Contour plots of the wavefront before and after the triplet was adjusted are shown in Figures 3-12 and 3-13, respectively. In the case of the original triplet, as published, (Figure 3-12) the contour interval is two wavelengths. The absence of contours near the center indicates a relative flatness of the wavefront across the center. The relatively narrow gap between contours near the edge of the plot indicates a greater curvature near the edge of the wavefront than near the center. The single erratic contour near the edge of the plot is probably due to diffraction. Figure 3-13 shows the contour plot of a wavefront emitted by the triplet after adjustment. The contour interval in this case is 0.200 wavelengths. Toward the center of the pattern the contours are regularly spaced indicating a relatively even curvature. Toward the edge, the distance between contours narrows indicating a more sharply curved wavefront. Unfortunately, from the plots of Figures 3-12 and 3-13 there is no way to determine the direction of curvature or if reversals of curvature occur.

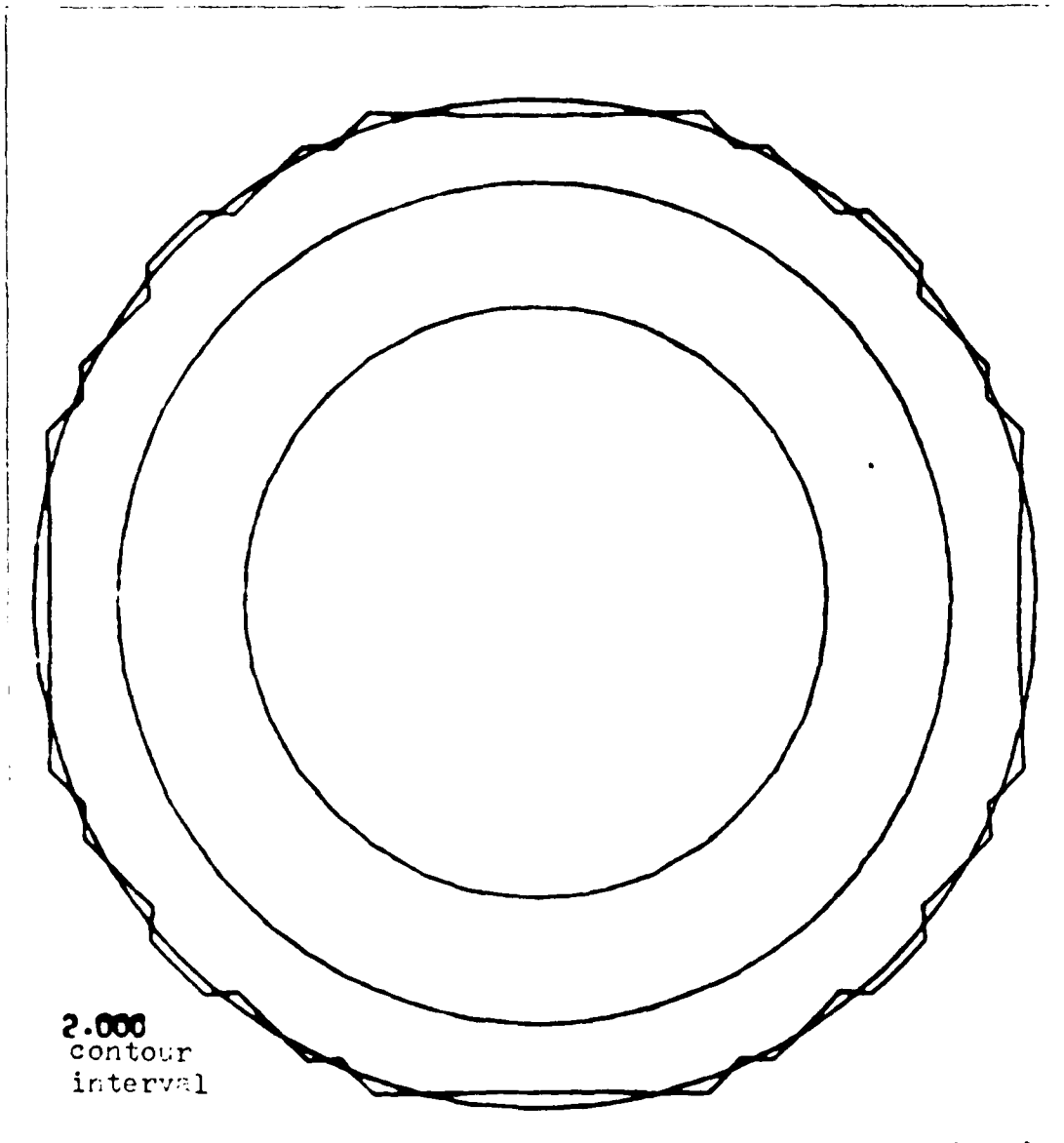


Figure 3-12. Wavefront Contour Plot for Original Triplet

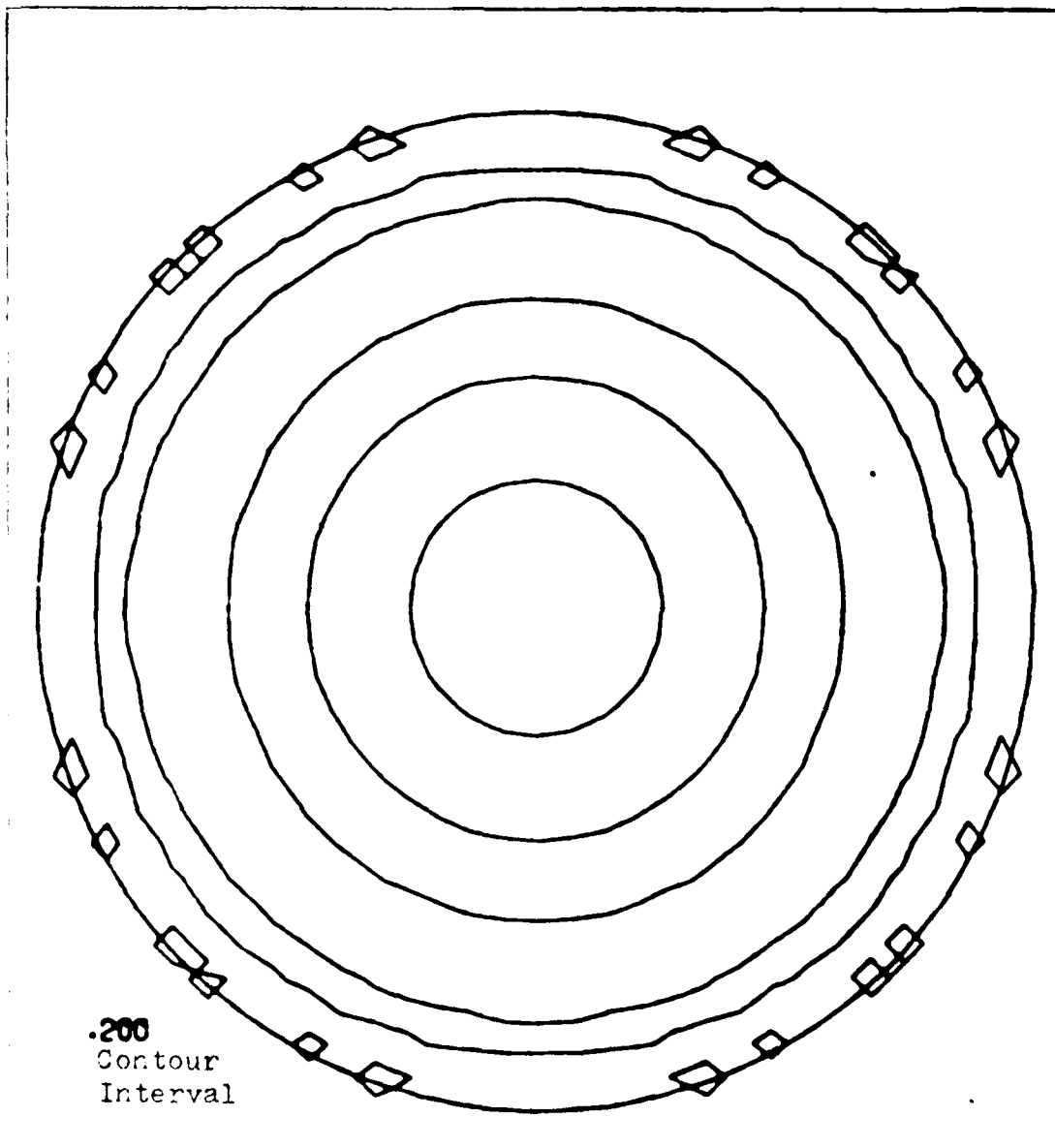


Figure 3-13. Wavefront Contour Plot for Adjusted Triplet

Isometric wavefront plots are shown in Figures 3-14 and 3-15 for the original and adjusted triplets, respectively. These plots remove the directional ambiguity inherent in the contour plots of Figures 3-12 and 3-13. Unfortunately

the FALCON code does not associate a scale with the isometric plots, but qualitatively used in conjunction with their respective contour plots they are very useful.

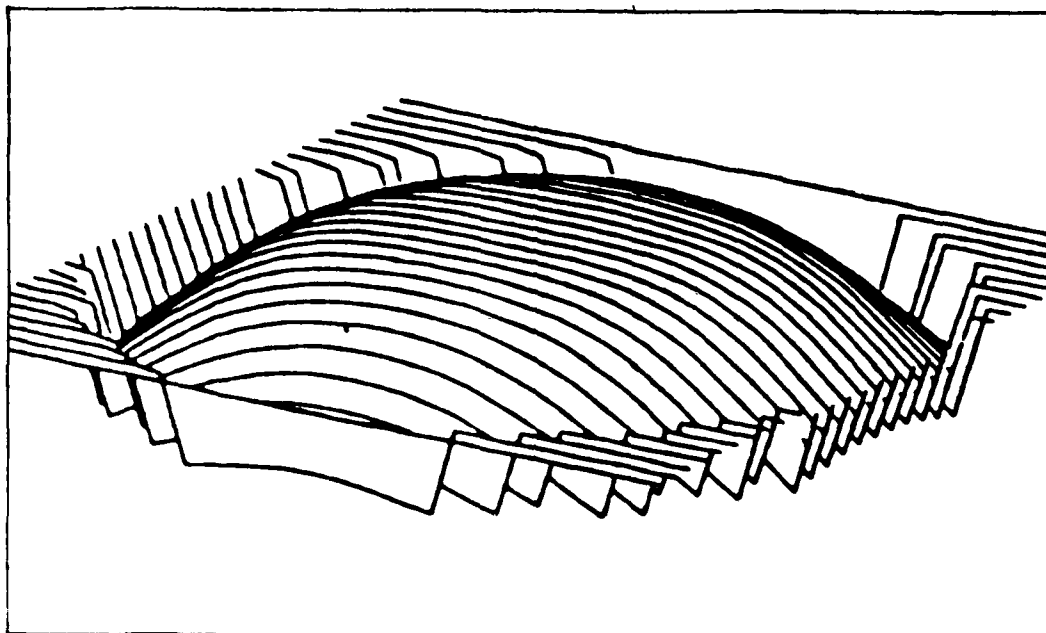


Figure 3-14. Isometric Wavefront Plot for Original Triplet

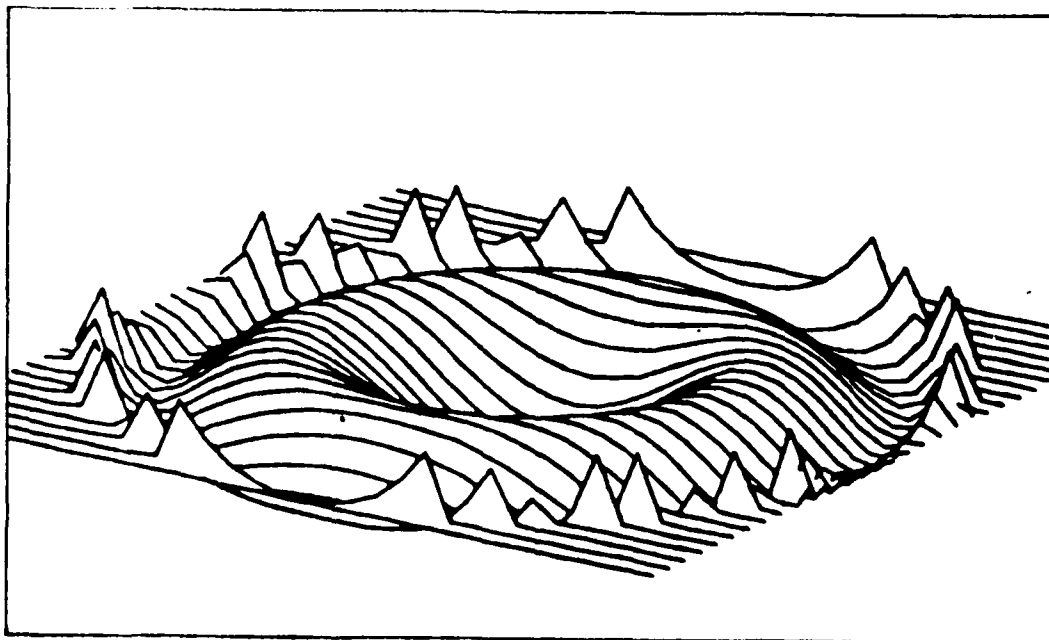


Figure 3-15. Isometric Wavefront Plot for Adjusted Triplet

The isometric plot of Figure 3-14 shows a distinct flatness across the center of the pattern as expected from examination of the contour plot alone. Figure 3-15, however yields a somewhat more surprising result for the case of the adjusted triplet. A dip is seen in the center of the wavefront which would not have been obvious from examination of the contour plot alone. The scaling of the isometric plot is such that this effect is very prominent. The jagged peaks around the edge of the pattern correspond to the irregular polygons that appear around the edge of the contour plot of Figure 3-13. They are a result of anomalies in the plot program and should be ignored.

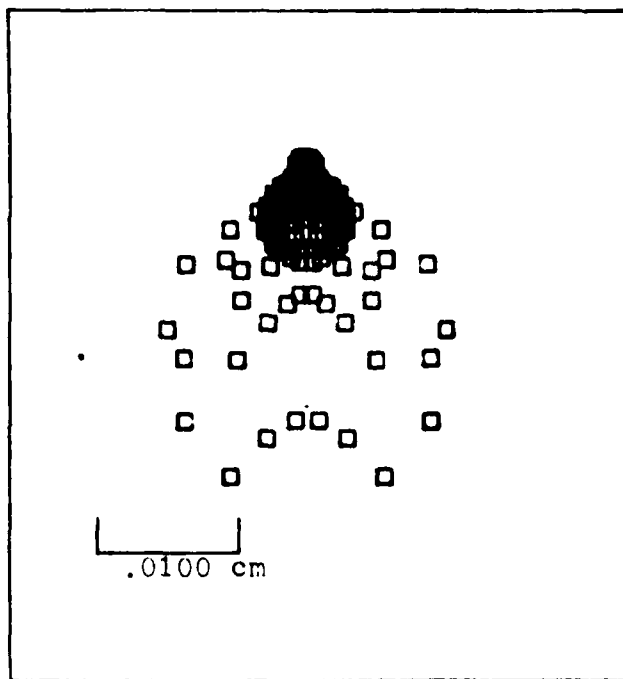


Figure 3-16. Spot Diagram for Decentered Triplet

In order to observe the effects of an off-axis object point, the adjusted triplet was decentered -1.25 cm from the

optical axis (-Y direction). The wavefront aberrations were seen to increase as shown in Table 3-2. This resulted in a reduction of the Strehl ratio to a point where the FALCON code could no longer calculate it.

A spot diagram was made for the decentered system and is

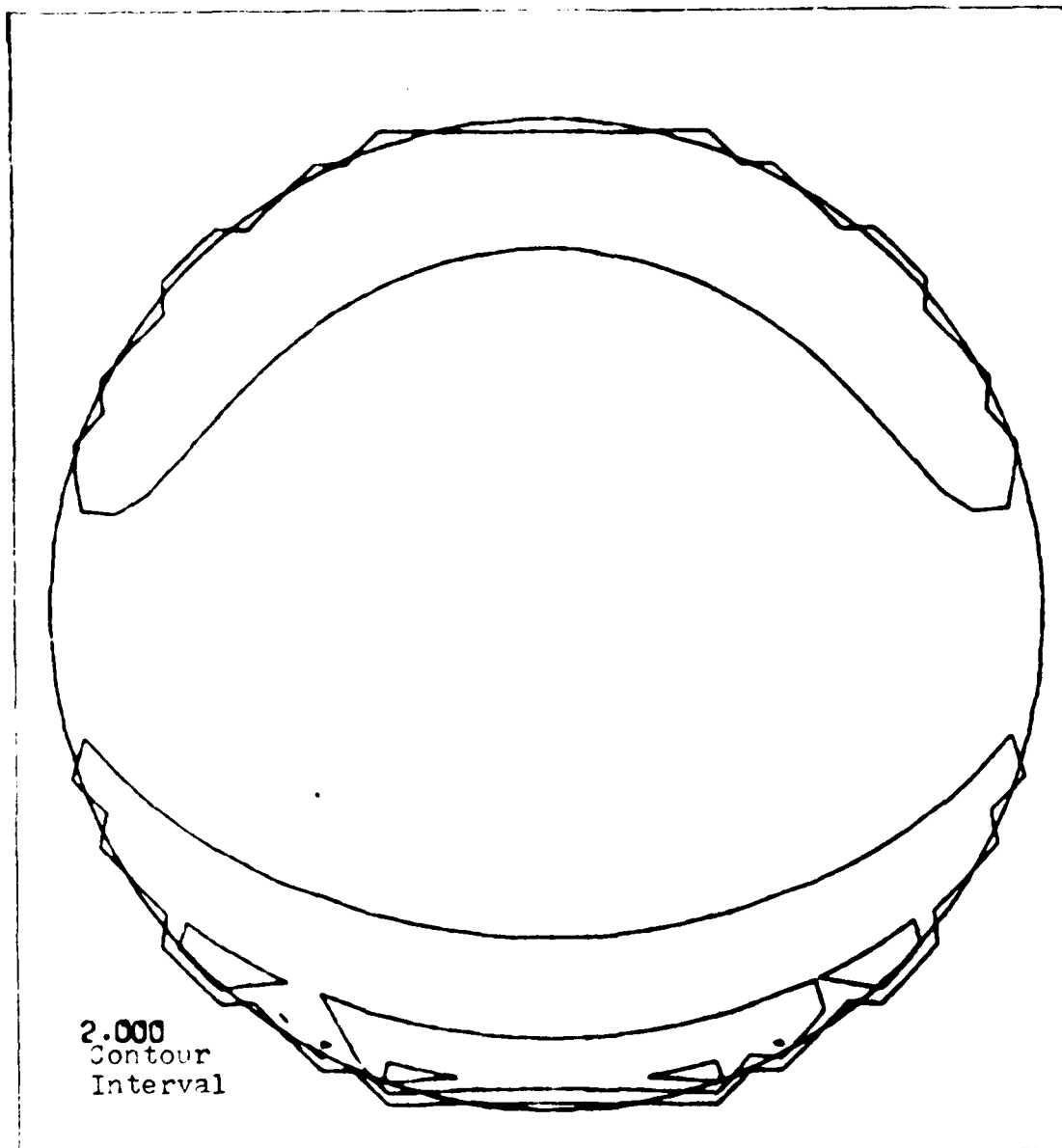


Figure 3-17. Contour wavefront Plot for Decentered Triplet

shown in Figure 3-16. The diagram shows a bright central spot with a diffuse tail. This shape is characteristic of the aberration, coma which typically results from tilted or off-axis configurations. In this case the radius of the central bright spot is approximately 0.007 cm. As expected, this is somewhat less tightly focused than the centered case due to the increased presence of aberrations.

The contour wavefront plot shown in Figure 3-17 and the isometric plot of Figure 3-18 show a dramatic distortion of the wavefront when compared to centered system of Figures 3-13 and 3-15. From the contour plot of Figure 3-17 it is

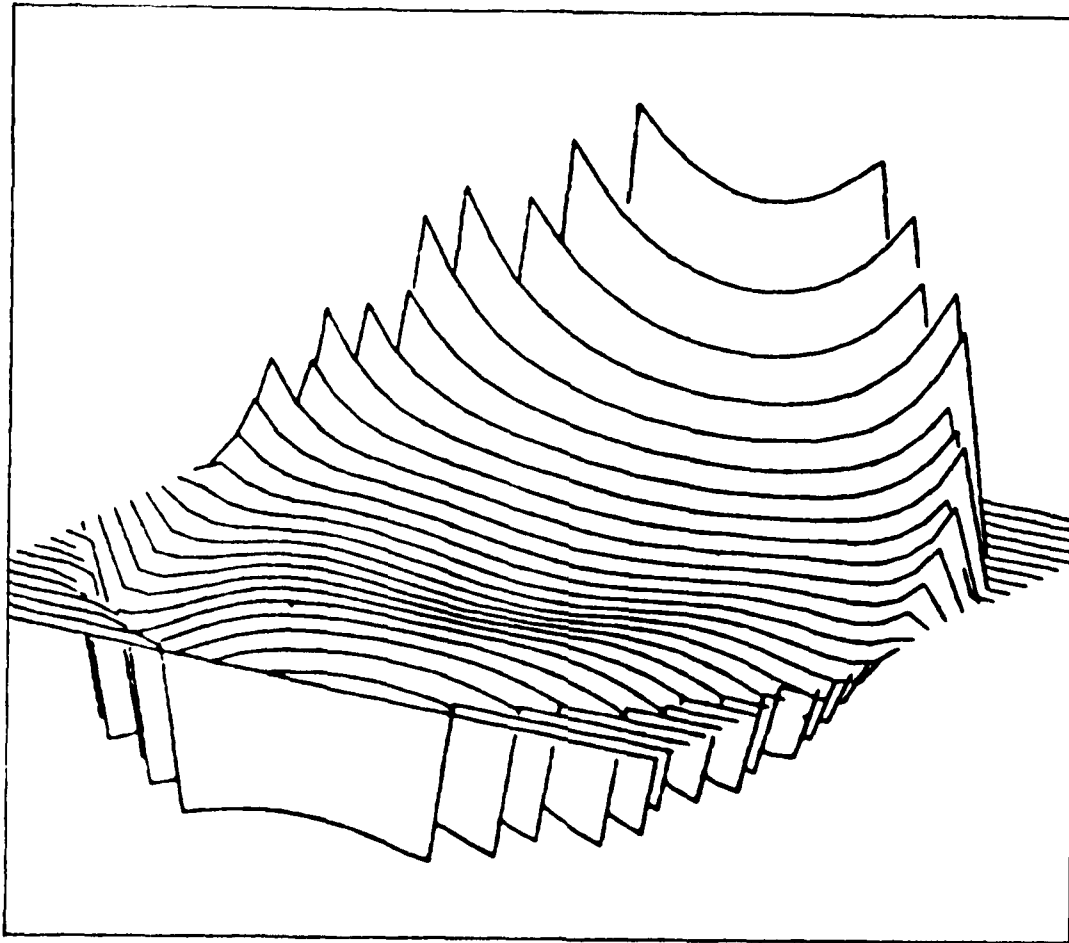


Figure 3-18. Isometric Wavefront Plot for Decentered Triplet

difficult to interpret the shape of the wavefront. With a contour interval of two wavelengths, much of the detail is obscured. The isometric plot of Figure 3-18, however, gives a good representation lending well to interpretation. The central depression that was present in the centered system is still present. The wavefront is also seen to tilt as verified by the tilt entry for the decentered system of Table 3-2.

The Cooke Triplet examined here allowed for the demonstration of several of the capabilities of the FALCON code. In addition, the manual calculations performed lend credence to the accuracy of the code's calculations and provide some insight into how the code determines values for various parameters. The original triplet was examined, adjusted, and re-examined in an effort to demonstrate changes resulting from small parametric adjustments. The system, after adjustment, was also decentered to demonstrate the effects of an off-axis object point on the aberrations present, the Strehl ratio, and the wavefront output by the system.

#### IV. THE DESIGN PROBLEM: OFF-AXIS BEAM EXPANDER

Reflective off-axis beam expanders have the advantage over centered systems that they avoid introducing an obscuration into the beam thus allowing the beam to remain contiguous (Ref 13:1141). For high power applications the irradiance of the laser beam often precludes the use of refractive optics. For high power applications where the use of refractive optics is ruled out, and where the beam is required to remain unobscured, the design solution often consists of an off-axis reflective system.

The major disadvantage in using off-axis geometries results from the tilting required of the surfaces to allow the beam reflected off one mirror to pass by the previous mirror unobstructed. By tilting the elements, aberrations are introduced that would not otherwise be present. This problem is elucidated by considering an ordinary on-axis optical system such as a microscope. By tilting only one element, the following defects are found in the center of the eyepiece: coma, astigmatism, distortion, field tilt, and lateral color (Ref 23:2169). Similarly, the tilts required in off-axis systems cause aberrations to be introduced into the system. The basis of the tilted component telescope (or beam expander) is simply that the objective mirror reflects the "axis" to the side where correcting elements can be employed without obstructing the light (Ref 23:2169).

From a practical point of view, rotationally symmetric

surfaces are preferred for off-axis systems. Rotationally symmetric surfaces produce beam expansion having uniform (with respect to the X and Y directions) magnification. The design studied here requires cylindrical optics to produce a different magnification in each of the two directions.

The design undertaken here arises from a requirement for an unobscured beam expander to be used on a continuous wave carbon dioxide laser proposed for construction at the Air Force Weapons Laboratory, Kirtland Air Force Base, NM (AFWL). The primary function of the beam expander is to receive as its input a 1.5 cm by 15 cm rectangular beam and to produce, as its output, a 12 cm by 12 cm square collimated output beam. Cylindrical elements were used because the system being considered receives a rectangular input and produces a square output (non-uniform magnification). Cylindrical mirrors are, by their shape alone, ideally suited to expand or compress a beam in the dimension perpendicular to the cylindrical axis leaving the dimension aligned with the cylindrical axis unaffected.

The beam expander is to be part of a ring laser system to be built to study the feasibility of implementing similar designs for use with a hydrogen fluoride laser system. The method of mixing molecular hydrogen and molecular fluorine to produce chemically excited HF produces a gain region whose cross sectional geometry is a rectangle of high aspect ratio. Thus, to efficiently extract energy from this gain region,

a long narrow rectangular beam is necessary. From diffraction considerations the beam divergence angle is given by the equation

$$\theta = 1.22 \lambda/D$$

where  $\lambda$  is the wavelength (in this case, 10.6 microns) and D is the aperture size (beam dimension). From the equation it is obvious that the narrow dimension of the unexpanded beam (D=1.5 cm) would lead to a greater divergence angle than the narrow dimension of the expanded beam (12 cm).

Optical systems used to transport the beam from the near field to the far field will usually be fabricated with X and Y dimensions of comparable magnitude (e.g. square or circular). The beam should therefore be expanded in such a manner as to fill the mirrors' apertures.

The system proposed by AFWL is in a conceptual stage with system constraints not yet well defined. As a result, several assumptions must be made to define and limit the design proposal. These assumptions include limiting the overall length of the six meters and allowing the mirror curvatures to assume any values governed only by the 6 meter overall length constraint. There were no upper limits placed on the aberration types and magnitudes that were tolerable; however, the goal was to achieve diffraction limited performance. It was from this point that the design proceeded.

The purpose of this design study is to successfully produce a design (or several designs) for an off-axis beam

expander to accept a 1.5 cm rectangular input beam and produce as its output a square 12 cm by 12 cm output beam.

System Description. The beam expander receives an output from the gain cavity in the form of a rectangular beam of dimensions 1.5 cm by 15 cm (X by Y). The first mirror, a diverging cylindrical mirror, the long axis of which is aligned with the Y axis, expands the narrow dimension of the beam (i.e. the X dimension) from 1.5 cm to approximately 12 cm at the surface of mirror 2. Mirror 1 has no effect on the Y dimension of the input beam. The input to mirror 2 is therefore a 12 cm by 15 cm rectangular beam. Mirror 2, a converging spherical mirror, collimates the beam in the X direction and converges the beam in the Y direction. Mirror 3, another diverging cylindrical mirror,

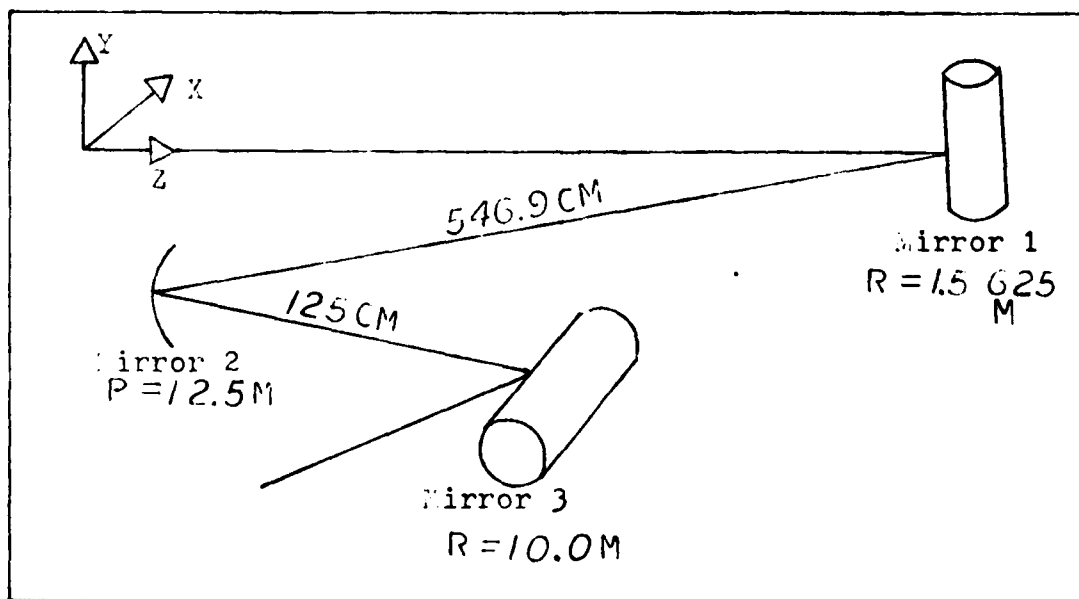


Figure 4-1. Beam Expander System Layout

is aligned along the X axis. This mirror has no effect on the collimated X dimension of the input beam, however it acts to collimate the beam in the Y dimension, producing a 12 cm by 12 cm square collimated beam. A system layout diagram is shown in Figure 4-1.

Design Constraints. The design began by placing some constraints on the system. First, in order to keep the overall size of the system within reason, an upper limit of six meters in overall length was chosen. In addition, since no optical components have been acquired to build the system, sizes of curvatures would be bound only by the arbitrary six meter restriction on the overall length of the system. As a first attempt, curvatures would be limited to cylinders and spheres without the use of higher order aspherics.

The General Design Approach. To begin, a first order analysis was performed using a short BASIC language routine. A listing is included in Appendix IV. The routine generated first order solutions for a system to receive a 1.5 cm by 15 cm input and produce a square 12 cm by 12 cm output. The routine is based on a matrix method first order solution (Ref 20:174) for which the focal length of mirror 3 was iteratively incremented. The BASIC code automatically adjusted the curvatures of mirrors one and two and the distances between the mirrors to produce a family of solutions. Using this approach, several hundred possible solutions were generated. Over a hundred of the previously generated solutions were screened using the FALCON code. In

the process, designs employing a converging cylindrical mirror as mirror 3, located beyond the focus of mirror 2, were found to yield categorically higher aberration coefficients than those designs using a diverging cylindrical mirror as mirror 3, located within the focus of mirror 2. As a result, the former design approach was discarded in favor of the latter. Eventually, the field was narrowed to a few possible solutions. The discarded designs were rejected primarily due to improper output dimensions, poorly collimated output, or the existence of larger aberrations than another solution. The reason that the first order analysis produced solutions whose outputs were not collimated or whose outputs were of incorrect dimensions is that for the first order analysis, the tilt angles were ignored and the system was effectively considered to be on-axis (without tilting or decentering).

A table of preliminary solutions leading to the final design is given in Table 4-1. Table 4-2 gives the wavefront aberrations and Strehl ratios as calculated by the FALCON ZPOLY LIST command for the solutions given in Table 4-1. Table 4-3 gives output beam dimensions and divergence angles for the solutions of Table 4-1. Table 4-2 shows a trend toward higher Strehl ratios and smaller wavefront aberrations as one proceeds toward solutions with larger distances between surfaces (proceeding downward on the table). Table 4-3 gives beam dimensions and divergence angles as calculated by the FALCON PARAX command. This was used to

distinguish "good" solutions from poorer ones having similar aberrations and Strehl ratios.

Preliminary Design Solutions

	Mirror Curvatures (1/cm)			Distances Between Surfaces (cm)	
	<u>Mirror 1</u>	<u>Mirror 2</u>	<u>Mirror 3</u>	<u>M1-M2</u>	<u>M2-M3</u>
1	.03200	.004000	.005000	109.4	25.0
2	.02133	.002667	.003333	164.1	37.5
3	.01600	.002000	.002500	207.8	50.0
4	.01280	.001600	.002000	273.4	62.5
5	.01067	.001333	.001667	328.1	75.0
6	.009143	.001143	.001429	382.8	87.5
7	.008000	.001000	.001250	437.5	100.0
8	.007805	.0009756	.001220	448.4	102.5
9	.007619	.0009524	.001190	459.4	105.0
10	.007442	.0009302	.001163	470.3	107.5
11	.007273	.0009091	.001136	481.2	110.5
12	.007111	.0008889	.001111	492.2	112.5
13	.006957	.0008696	.001087	503.1	115.0
14	.006809	.0008511	.001064	514.1	117.5
15	.006667	.0008333	.001042	525.0	120.0
16	.005631	.0008163	.001020	535.9	122.5
17	.006400	.0008000	.001000	546.9	125.0

Table 4-1. Preliminary Design Solutions

Paraxial Output Beam Parameters

	Beam Half-Dimension(cm)		Divergence Angle (rad)	
	<u>Y</u>	<u>X</u>	<u>Uy</u>	<u>Vx</u>
1	6.000000	5.999040	.000000	.000010
2	5.997760	5.997761	.000010	.000011
3	6.000000	6.000000	.000000	.000005
4	6.000001	5.999885	.000000	.000002
5	6.002426	6.002806	-.000010	-.000006
6	6.000306	5.999538	-.000002	.000001
7	6.000001	6.000000	.000000	.000000
8	6.001223	5.999945	.000006	.000001
9	5.998754	6.000015	.000006	.000001
10	6.000678	6.000167	.000003	-.000001
11	5.999079	5.999941	.000005	.000001
12	5.999674	5.999929	.000002	.000000
13	5.999915	6.000140	.000000	.000000
14	6.000210	6.000445	-.000001	.000001
15	6.000986	6.000411	.000005	.000000
16	5.999169	6.000264	.000004	.000001
17	6.000001	6.000115	.000000	.000000

Table 4-2. Paraxial Output Beam Parameters

Aberrations and Strehl Ratios for Preliminary Solutions

(aberrations measured in wavelengths at 10.6 microns)

	<u>Tilt</u>	<u>Defocus</u>	<u>Astig.</u>	<u>Coma</u>	<u>S.A.</u>	<u>Strehl Ratio</u>
1	.396	1.346	.047	.362	.209	.528
2	.176	.756	.064	.161	.062	.881
3	.099	.654	.075	.090	.026	.959
4	.063	.509	.052	.058	.013	.983
5	.044	.493	.010	.040	.008	.992
6	.032	.358	.010	.029	.005	.996
7	.025	.307	.026	.023	.003	.997
8	.024	.335	.001	.021	.003	.998
9	.022	.257	.052	.020	.003	.997
10	.021	.305	.011	.020	.003	.998
11	.020	.260	.051	.019	.002	.997
12	.020	.262	.029	.018	.002	.998
13	.019	.266	.024	.017	.002	.998
14	.018	.263	.010	.016	.002	.999
15	.017	.281	.000	.016	.002	.999
16	.016	.232	.019	.015	.002	.998
17	.016	.243	.019	.014	.002	.999

Table 4-3. Aberrations and Strehl Ratios

The Final Design. The lens deck for the final design is listed in Table 4-4.

```
0 SAY 7.5 SAX .75 TH 1E10 WV 10.6 AFOCAL
1 TH 200 CLAP 7.5 .75 RECT
2 REFL TILT 1.5 TH -546.9 CV .0064 CVX
3 CV .0008 REFL TILT -3 TH 125 DEC -14.316
4 REFL TH -200 DEC -9.81 TILT 2 CV .001 CVY
5 END
```

Table 4-4. Beam Expander Input

In line 0 above, the object is described by axial rays in the X direction at .75 cm and in the Y direction at 7.5 cm. The FALCON code interprets this as an object symmetric about the X and Y axes. The true size of the object is then interpreted by the FALCON code as 1.5 cm by 15 cm. The distance between the object and the surface following is specified as  $10^{10}$  cm. This is the maximum distance permitted and is used to provide an essentially collimated input. The system is designated as afocal, indicating a collimated output. This causes the FALCON code to output aberration coefficients in angular measure. This will be discussed in some detail later. Surface 1 is specified as a clear aperture, centered on the Z axis, with an X half-dimension of .75 cm and a Y half-dimension of 7.5 cm. The distance between this surface and the following one is specified as 200 cm. Line 2 describes mirror 1 as shown in Figure 4-1. The mirror curvature (i.e. the reciprocal of

the radius of curvature) is specified as .0064 cm. The surface is tilted 1.5 degrees counterclockwise as specified by the Euler angles described in chapter II. The distance between mirrors 1 and 2 given as 546.9 cm. The identifier CVX identifies the surface as a cylinder, the long axis of which is aligned with the Y axis. Mirror 2, the spherical mirror, is described in line 3. The DEC identifier indicates that mirror 2 is decentered from the local Z axis of mirror 1 by -14.316 cm. The remaining parameters are as described for the preceding surface. Mirror 3 is described in line 4. The CVY parameter without identifiers indicates a cylindrical

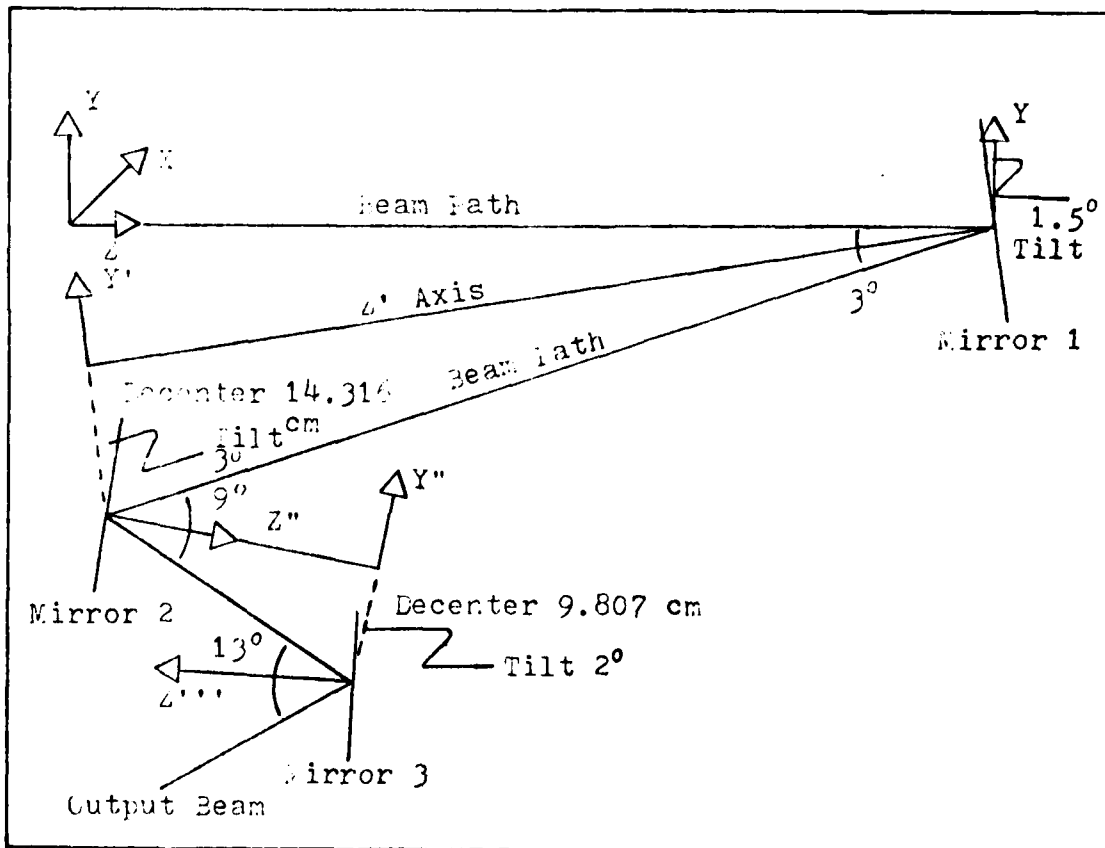


Figure 4-2. Tilts and Decenters

element, the axis of which is aligned with the X axis. All remaining parameters are as described for previous surfaces.

The final design is shown diagrammatically in Figure 4-1. Mirror 1 is a diverging cylindrical mirror with a radius of curvature of 156.25 cm. The local Y and Z axes of mirror 1 are tilted 1.5 degrees counterclockwise with respect to the original Y and Z axes, respectively. This produces an angle of 3 degrees subtended by the on-axis incident and reflected beams at mirror 1. Mirror 2 is separated from mirror 1 by 546.9 cm. Mirror 2 is a converging spherical mirror with a radius of curvature of 12.5 meters. Mirror 2 is tilted 3 degrees clockwise with respect to the Y axis, in the local YZ plane of mirror 1. This causes the incident and reflected on-axis rays at mirror 2 to subtend an angle of 9 degrees. The distance between mirror 2 and mirror 3 is 125 cm. Mirror 3 is a diverging cylindrical mirror with a radius of curvature of 10 meters. Mirror 3 is tilted 2 degrees counterclockwise with respect to the Y axis, in the local YZ plane of mirror 2. This causes the incident and reflected on-axis rays at mirror 3 to subtend an angle of 13 degrees. The output of the system is a collimated rectangular beam with a Y dimension of 12.00002 cm and an X dimension of 12.00023 cm.

Tilt angles and decenters are shown in Figure 4-2. The beam path initially follows the Z axis until it reaches mirror 1. Mirror 1 is tilted 1.5 degrees counterclockwise with respect to the original Y axis. The new Z axis, labeled

Z', is defined normal to the tilted mirror 1. The Z' axis subtends an angle of 1.5 degrees with the Z axis and also with the incident beam. This causes the beam to strike mirror 1 with an angle of incidence of 1.5 degrees. By the Law of Reflection, the angle subtended by the incident and reflected beams at mirror 1 is 3 degrees. From mirror 1 the beam travels 546.9 cm to mirror 2. Mirror 2 is displaced from the Z' axis by 14.316 cm ( $546.9 \sin 1.5^\circ$ ) in order for the beam to strike its center. If mirror 2 were left perpendicular to the Z' axis (tilt = 0) the beam would strike mirror 2 at an incident angle of 1.5 degrees. Mirror 2, however, is rotated 3 degrees clockwise making the incident angle 4.5 degrees. By the Law of Reflection, the angle subtended by the incident and reflected beams at mirror 2 is 9 degrees. The new Z" is axis defined by the normal to mirror 2. From mirror 2 the beam travels 125 cm to mirror 3. Mirror 3 is displaced from the Z" axis by 9.807 cm ( $125 \sin 4.5^\circ$ ) in order for the beam to strike its center. If mirror 3 were left untilted, the beam would strike it at an incidence angle of 4.5 degrees. Mirror 3 is, however, rotated 2 degrees clockwise causing the incidence angle to increase to 6.5 degrees. Therefore, by the Law of Reflection, the incident and reflected beams at mirror 3 subtend an angle of 13 degrees.

Angular Aberrations. An alternative to using linear measure to describe amounts of aberration is to describe them using angular measure. If in a focal optical system

no aberrations were present, all rays would pass through the paraxial focus. Aberrations within the system can then be thought of as causing the rays beyond the strictly paraxial zone to take an undesirable or wrong direction. The angular difference between the real direction and the ideal direction is a legitimate measure of aberration (Ref 16:116).

This measure of aberrations is particularly well suited for afocal systems where angular deviations are measured with respect to the ideal, perfectly collimated output. This is the means by which the FALCON program calculates Seidel aberrations for afocal systems. The sign convention dictates that positive angular aberrations result from clockwise angular displacements.

Design Analysis. The final design consists of two diverging cylindrical mirrors surrounding a single converging spherical mirror. Without the use of conic and higher order aspherics, a Strehl ratio of 0.999 was achieved. Using the method of Buchdahl (Ref 10), third and fifth order aberrations were calculated. The final design resulted in all third and fifth order aberrations being less than 0.9 mrad. These results lend themselves less well to interpretation than the wavefront aberrations calculated using the FALCON's ZPOLY LIST command. By fitting a set of Zernike Polynomials to the optical path difference data in the ray matrix file (generated by the PUPIL command), the wavefront aberration  $\phi$ , is calculated. The output of the ZPOLY LIST command is summarized in Figure 4-3. The first table of Figure 4-3

gives the root mean square (rms) fit, in wavelengths, for different orders of Zernike polynomials. As is shown by the data, the rms wavefront fit using up to sixth order polynomials does not deviate by more than 0.001 wavelengths. The next table gives fourth order wavefront aberrations with none exceeding one quarter of a wavelength. The last table indicates the contribution of different orders to the total spherical aberration. The column labeled "ZERNIKE" lists the radial Zernike polynomials used. The column labeled "ASPHERIC" lists the corresponding coefficients for the following expansion:

$$z = c_0 + c_2 r^2 + c_4 r^4 + c_6 r^6 + \dots \quad (4-1)$$

These coefficients are obtained by uncoupling different powers of  $r$  in the Zernike radial polynomial expansion. The Strehl ratio is calculated to be .999 indicating a reduction in intensity at the diffraction focus of 0.1 percent. This is substantially under the 20 percent criterion discussed in Appendix III.

Figure 4-4 shows a contour plot of the output wavefront with a contour interval of 0.04 wavelengths (0.42 microns at  $\lambda = 10.6$  microns). Figure 4-5 gives an isometric plot of the same wavefront. Figures 4-4 and 4-5 both show a very nearly spherical wavefront with no major irregularities. Although quantitatively these plots are not terribly useful, as a qualitative means they are very useful in readily detecting irregularities in the transmitted wavefront.

FIELD ANGLE 0.0 DEG

BILATERAL SYMMETRY INVOKED

	TERMS	RMS
	0	.030
TILT	1	.030
FOCUS	2	.005
4TH ORDER	5	.003
6TH ORDER	9	.000
8TH ORDER	14	.000
10TH ORDER	21	NEGATIVE VARIANCE

STREHL RATIO .999 AT DIFFRACTION FOCUS

FOURTH ORDER ABERRATIONS

MAGNITUDE	ANGLE	DESIGNATION
.016	90.0	TILT
.243		DEFOCUS
.019	0.0	ASTIGMATISM
.014	90.0	COMA
.002		SPHERICAL ABERRATION

RADIAL COEFFICIENTS

ORDER	ZERNIKE	ASPHERIC	RAYS
2	.121	.242	.000484
4	.000	.000	.000001
6	-.000	.000	.000000
8	.000	-.000	.000000
10	-.000	.000	.000000
12	-.000	-.000	-.000000

Figure 4-3. ZPOLY LIST Output Summary

The spot diagram of Figure 4-6 demonstrates the square dimensions of the beam and the uniformity of the intensity

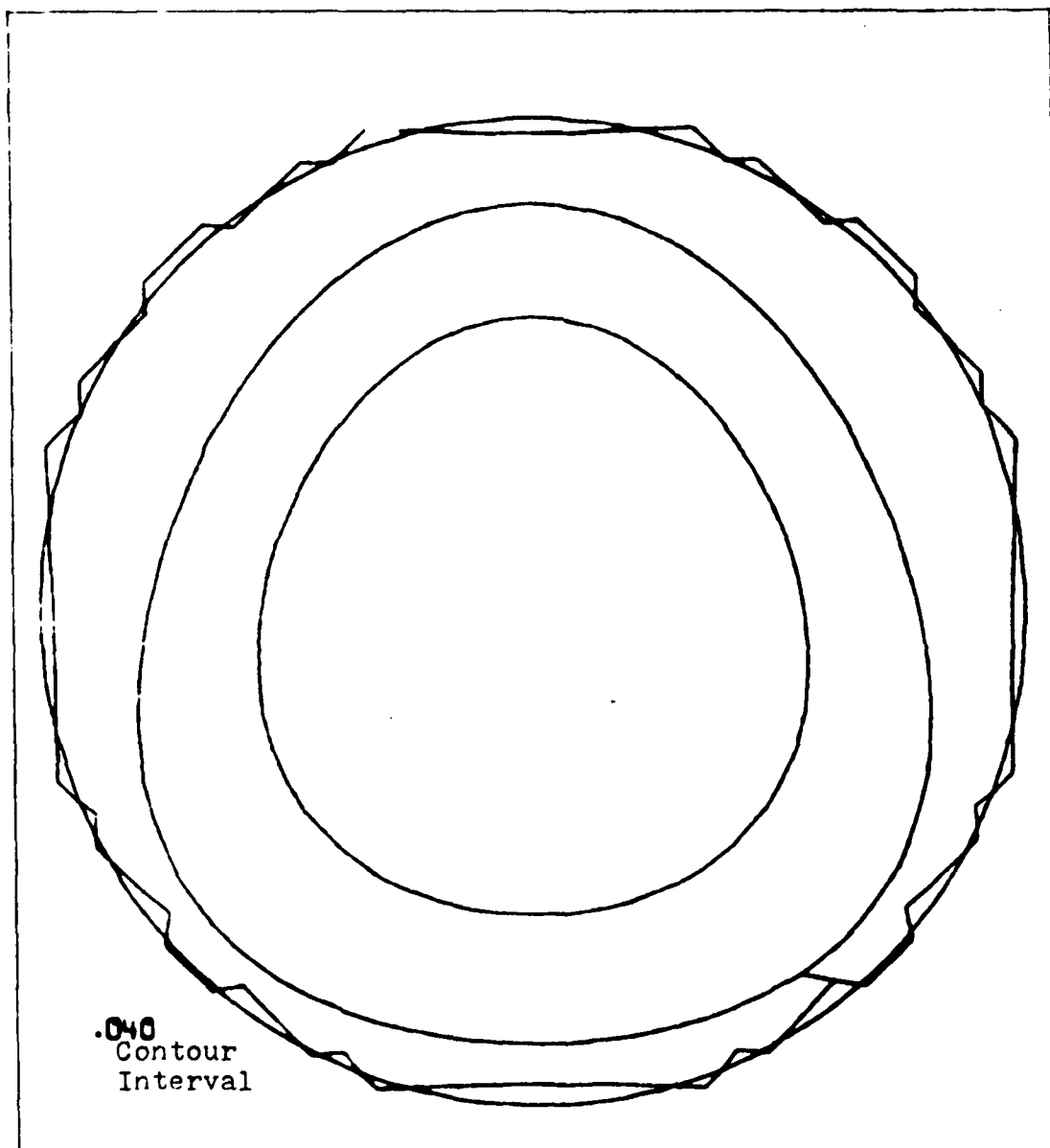


Figure 4-4. Wavefront Contour Plot

distribution. This diagram is taken in the focal plane (designated 200 cm to the left of mirror 3) by tracing a uniform grid of parallel rays on the surface of mirror 1, through the system. For the diagram shown in Figure 4-6, approximately 1000 rays are shown. The output shows the uniformity of the intensity distribution across the output beam.

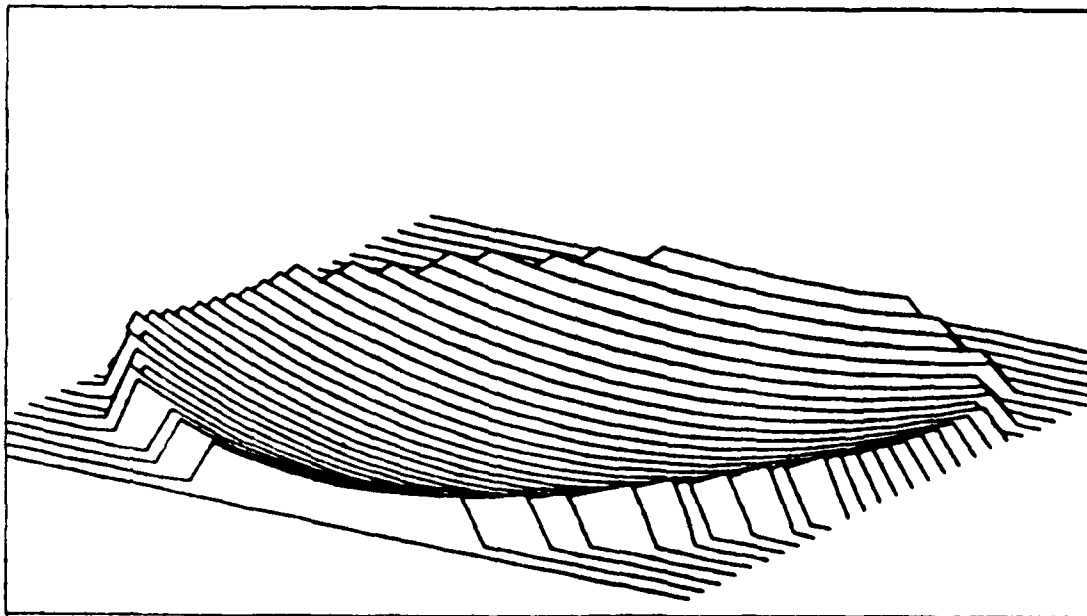


Figure 4-5. Isometric Wavefront Plot

The design presented here meets the functional requirements of the beam expander described by AFWL. The Strehl ratio of 0.999 exceeds the accepted diffraction limited criterion of 0.80 for an operating wavelength of 10.6 microns. The final design was chosen as the best of those considered on the basis of its wavefront aberration coefficients as generated by the ZPOLY LIST command and on the Strehl ratio calculated using the same command. In

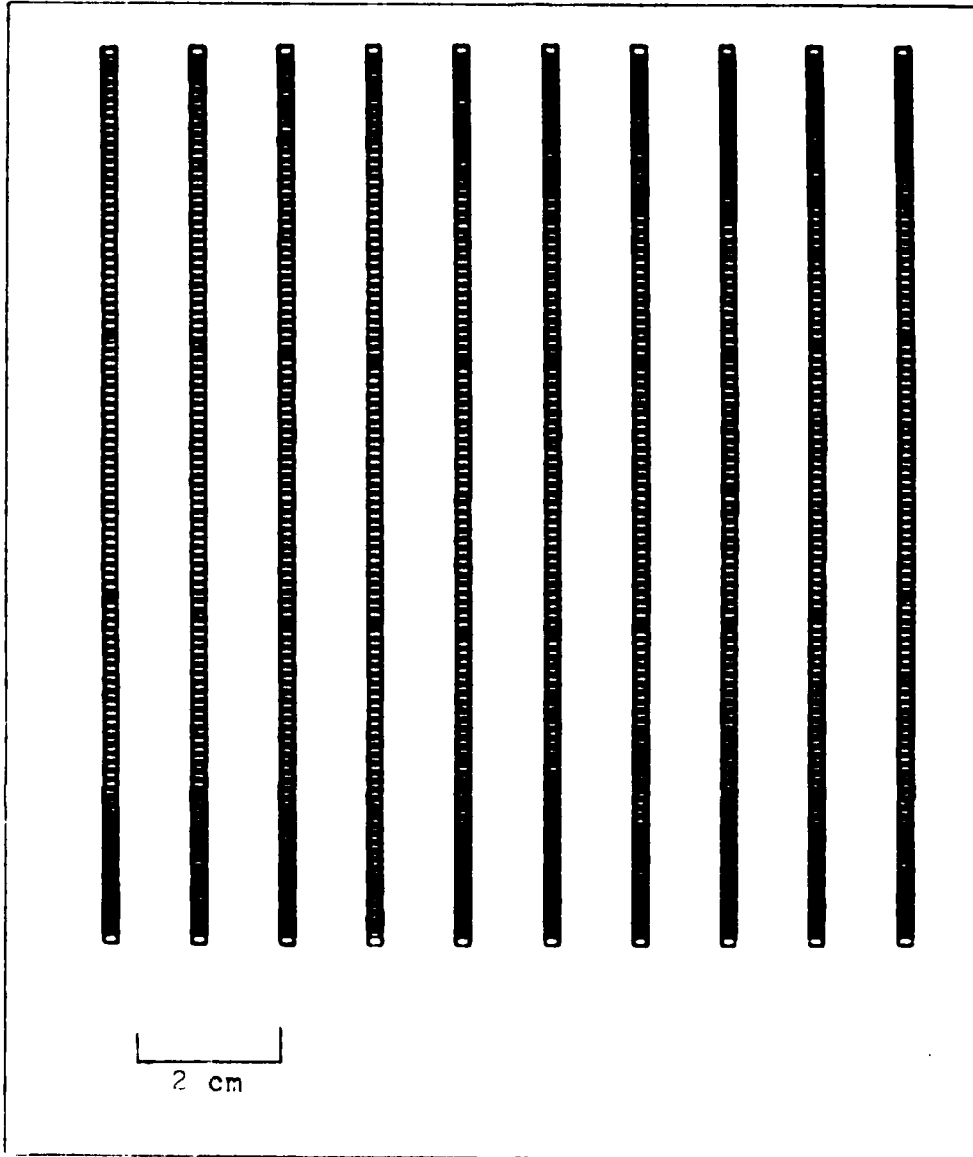


Figure 4-6. Spot Diagram

cases where there was no clear reason to choose one solution over another on these bases, the dimensional data of Table 4-3 were taken into account. Those solutions whose dimensions were closest to 12 cm by 12 cm and with divergence angles

nearest to zero were chosen above others.

From a comparison of the corresponding solutions from Tables 4-1 and 4-3 an evolution of progressively better solutions (lower aberrations, higher Strehl ratios) is shown to correspond with larger distances and with smaller curvatures. In general less abruptly curved mirrors imply smaller aberrations and this is shown here. In tables 4-1, 4-2, and 4-3, the solution numbered 17 is the solution chosen as the final design. This solution was chosen above all others examined because it offered both a Strehl ratio of .999 and low wavefront aberrations. Of those possible solutions examined with a Strehl ratio of .999, this particular solution yielded output dimensions closest to 12 cm by 12 cm (actually 12.000002 by 12.000230) with the smallest divergence angles (less than 1 microradian).

For systems with 30 percent less separation between mirrors, and radii of curvature 30 percent shorter than the final design solution described above, Strehl ratios of greater than 0.990 can be achieved with output beam divergence angles less than 5 microradians (Solution 6, Tables 4-1, 4-2, and 4-3).

## VI. CONCLUSION

The objectives of this these were many-fold. The first and most important purpose was to learn about computer aided geometrical optics design to the point where a design task could be undertaken and accomplished. This included the analysis of a Cooke triplet as an exercise of the FALCON code. It also included the design of a beam expander, the requirement for which arose from a need at the AFWL. In addition to accomplishing these tasks, some of the theory upon which the FALCON code is built was also examined. Also considered were the ideas of optical tolerance and aberration control.

### Triplet Analysis

A Cooke triplet was analyzed as a demonstration of the FALCON code. The summary of the results of that analysis is presented here.

For the original triplet, as published, the Strehl ratio was calculated to be 0.235. The dominant third order aberration was spherical aberration at -2.203 wavelengths ( $\lambda=0.58756$  microns). An adjustment was made to the triplet in an attempt to reduce the spherical aberration by slightly adjusting the focus. This was accomplished by reducing the distance between the second and third elements from 1.13691 cm to 1.07600 cm. After this adjustment was made, the focal plane was moved from 14.05015 cm to 14.15522 cm to the right of surface 6. This reduced the defocus from -9.999 wave-

lengths to 0.000 wavelengths. After reducing the distance between elements two and three but before moving the focal plane, the spherical aberration was calculated to be 0.067 wavelengths. The Strehl ratio was 0.648. After moving the focal plane, defocus was reduced to 0.000, however a small increase in spherical aberration from 0.067 to 0.078 was observed. The Strehl ratio remained at 0.648. In all cases, the object was positioned 25 cm to the left of the first element.

The spot diagram showed a central bright spot for the original triplet with a diameter of 0.014 cm which, after adjustment, was reduced to 0.0020 cm. As expected, the spot size should reduce with a reduction in aberrations.

When the adjusted system was decentered -1.25 cm (-Y direction) off the optical axis to examine the effects of an off-axis object point, the dominant third order aberration became coma at 1.768 wavelengths. The object position remained at 25 cm as before. The spot diagram showed a comet-like pattern with an intense head and a more diffuse tail region which is characteristic of the aberration coma. The diameter of the central bright spot increased from approximately 0.0020 cm for the centered system, to 0.0096 cm for the decentered system. For more highly aberrated system configurations, the size of the focal spot is expected to be larger, as observed.

#### Off-Axis Beam Expander

The function of the off-axis beam expander considered

in this effort is to receive, as its input, a 1.5 cm by 15 cm rectangular laser beam, and produce as its output, a 12 cm by 12 cm rectangular beam. The design solution proposed by the AFWL utilized two cylindrical mirrors and a single spherical mirror. Upon analysis it was found that solutions employing two diverging cylindrical mirrors produced categorically lower aberrations than solutions employing one diverging cylindrical mirror and 1 converging cylindrical mirror. As a result, the former approach was chosen over the latter. The design solution chosen was the best solution examined based on Strehl ratios and output beam parameters. The Strehl ratio was calculated to be 0.999 with the dominant aberration being astigmatism at 0.019 wavelengths ( $\lambda = 10.6$  microns). The output beam divergence is less than one microradian in both X and Y dimensions. The dimensions of the output beam are 12.000020 cm in the Y direction by 12.00023 cm in the X direction. Wavefront plots show an absence of irregularities and the spot diagram shows an even distribution of intensities across the beam.

#### Recommendations

The avenues open in the field of geometrical optics design for further investigation are too numerous to discuss here; however, several issues of interest surfaced through the course of this effort. When thinking of computer aided optical design, the question of division of labor arises.

How much of the design can be done by the computer and how much must be done by the designer? Of particular interest is the use of optimization techniques to produce a best possible design. A survey of currently used optimization techniques and an application to a simple design could be performed (Ref 24:66). Furthermore, it would prove insightful to examine conditions under which several optimization techniques fail to perform adequately (Ref 25:75).

Another possibility for a later effort, in order to gain a working knowledge of optical design, might involve studying a relatively simple optical system (e.g. a triplet). A detailed analysis of the effects of several parametric adjustments would provide for an interesting study with the added possibility of gaining insight into design cause and effect. Such an effect would involve studying the effects of changes in surface curvature and refractive index as well as inter-element distance on the magnitudes of third order aberrations. The inclusion of apertures and their positioning in the system as it effects system performance should also be considered.

## Bibliography

1. Kingslake, Rudolph. "Lens Design Without a Computer", Computer Aided Optical Design, SPIE 147: 58.
2. Loomis, John. FALCON Version Two User's Manual. Ohio: University of Dayton, 1981.
3. Military Standard Handbook, Optical Design. Washington D.C.: U.S. Government Printing Office, 1962.
4. Born, Max and Emil Wolf. Principles of Optics. New York: Pergamon Press, 1975
5. Lea, Michael. Geometrical Optics. Rochester: Institute of Optics, University of Rochester, 1982.
6. Longhurst, Richard S. Geometrical and Physical Optics. London: Longmans, Green and Co, 1957.
7. Buchdahl, Hans A. Optical Aberration Coefficients. London: Oxford University Press, 1954.
8. Welker, William J. An Application of a Computer Optical Design Program (Thesis). Air Force Institute of Technology, 1982.
9. Kingslake, Rudolph. Applied Optics and Optical Engineering, Volume III. New York: Academic Press, 1965.
10. Erkkila, John H. Notes on Diffraction Theory of Aberrations. Air Force Institute of Technology, (unpublished).
11. Kingslake, Rudolph. Lens Design Fundamentals. New York: Academic Press, 1978.
12. Welford, W.T. Aberrations of the Symmetrical Optical System. New York: Academic Press, 1974.
13. Gelles, Robin. "Unobscured Aperture Two-Mirror Systems", Journal of the Optical Society of America, 65: 1141-1143.
14. Loomis, John S., "The Use of Paraxial Solves in Lens Design", Computer Aided Optical Design, SPIE 147: 6
15. Hecht, Eugene and Alfred Zajac. Optics. Reading Massachusetts: Addison-Wesley, 1974.

16. Conrady, Alexander E. Applied Optics and Optical Design. London: Oxford University Press, 1942.
17. Swartzchild. Untersuchungen Zur Geometrischen Optik Vol. III. Berlin: Weidmann, 1905.
18. Baker, James G. "Explorations in Design", Computer Aided Optical Design, SPIE 147: 102.
19. Irving, Bruce R. "Diffraction Evaluation of the General Optical System", Computer Aided Optical Design SPIE 147: 19.
20. Shafer, David. "Design With Two Axis Aspheric Surfaces", Computer Aided Geometrical Optics Design, SPIE 147: 171.
21. Robb, Paul N. "Lens Design Using Optical Aberration Coefficients", Proceedings of the Society of Photo-Optical Instrumentation Engineers", SPIE 237:109.
22. King, W.B. "Unobscured Laser Beam Expander Pointing System with Spherical Mirrors", Applied Optics 13:21.
23. Buchroeder, R. A. "Tilted Component Telescopes. Part I: Theory", Applied Optics 9:2169.
24. Harrigan, Michael E. "New Approach to the Optimization of Lens Systems", Proceedings of the Society of Photo-Optical Instrumentation Engineers, SPIE 237:66.
25. Rayces, Juan L. "Ten Years of Lens Design with Glatzel's Adaptive Method", Proceedings of the Society of Photo-Optical Instrumentation Engineers, SPIE 237:75.

## Appendix I

### Glossary

Axial Ray - That ray which begins at the on-axis object point and passes through the optical system. For focal systems, the image is located where the axial ray crosses the optical axis.

Chief Ray - That ray starting at an off-axis object point, which passes through the center of the aperture stop.

Diffraction Focus - When aberrations are present in a focal system the diffraction focus is the point of maximum intensity in image space.

Gaussian Focus - In the absence of aberrations in a focal system, the point of maximum intensity in image space is the Gaussian focus.

Gaussian Reference Sphere - In the absence of aberrations in a focal system, the imaginary sphere whose center is located at the image of an object point in the Gaussian focal plane. The Gaussian Reference Sphere passes through the point of intersection of the exit pupil plane with the optical axis.

Sagittal Plane - The plane which contains the chief ray and is perpendicular to the tangential plane throughout the optical system.

Tangential Plane - The plane containing the off-axis object point and the optical axis; throughout the optical system, the chief ray lies in the Tangential plane.

## Appendix II

### Running FALCON

Running the FALCON code interactively is a simple matter requiring a few preparatory steps. These steps are described below to expedite the process for users that may follow.

The FALCON code is written for use on CDC Cyber computers with a Tektronix graphics terminal. The Tektronix 4025 terminal requires that the following commands be entered in order to display the graphics generated by the FALCON code:

```
:WOR 33H
:GRA 1,35
:SHRINK
```

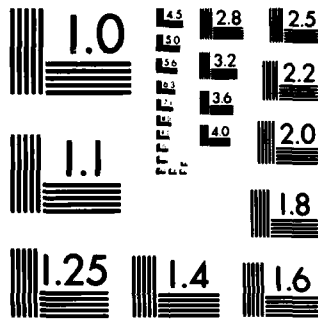
Large format tektronix terminals do not require these terminal commands. The colon preceding the verbal portion of the command is the terminal control character and may vary from one terminal to the next.

Once logged in on the Cyber computer, the following sequence should be entered upon receiving the COMMAND-prompt from the Cyber:

```
ATTACH,LFN1, FALCON,ID=_ _ _ _ _
ATTACH,LFN2,OPTLIB,ID=_ _ _ _ _
CONNECT,INPUT,OUTPUT
LFN1
```

The quantities LFN1 and LFN2 are local file names of the operators own choosing. The ID=\_ \_ \_ \_ \_ may be omitted if





MICROCOPY RESOLUTION TEST CHART  
NATIONAL BUREAU OF STANDARDS-1963-A

the operator has copies of the FALCON and OPTLIB codes in files under the same ID number as that used to LOGIN.

This sequence should start the FALCON program. In order to initiate the graphics mode within FALCON, the command SYSTEM TEK ON must be entered.

### Appendix III

#### DIFFRACTION THEORY OF ABERRATIONS

Contained in this appendix is a brief discussion of the diffraction theory of aberrations. To this end, Zernike polynomials, aberration balancing, and aberration tolerances are all discussed. In doing geometrical optics designs, an understanding of the diffraction effects, although not specifically considered, is essential to the understanding of aberration balancing and tolerances. In addition, the FALCON program uses Zernike polynomials to calculate wavefront aberrations, the understanding of which is the cornerstone in balancing aberrations.

For an ideal optical system without aberration, each object point has a distinct image point in the Gaussian image plane. If the effects of diffraction are taken into account, the image appears as a complex diffraction figure, the form of which depends on the shape of the exit pupil. The point spread function for a clear circular aperture is the familiar Airy pattern, the intensity distribution for which is given by

$$I(r) = (2J_1(v)^2)/v^2 \quad (3-1)$$

where

$$v = (2\pi arn)/\lambda R$$

In this equation  $r$  is the radial distance from the center of the pattern,  $R$  is the radius of the reference sphere,  $a$  is the radius of the exit pupil,  $\lambda$  is the wavelength of light,

$n$  is the refractive index, and  $J_1$  is a Bessel function of first order (Ref 8:34). The equation is normalized such that the intensity at the center of the pattern is unity and thus, the quantity  $I(r)$  is dimensionless. For a focal system, if the effects of diffraction are ignored for the present the equation for a converging spherical wavefront can be written as

$$\epsilon = \epsilon_0 \text{EXP}[-ik(x_e^2 + y_e^2)/2R] \quad (3-2)$$

where  $x_e$ ,  $y_e$  are the coordinates in the exit pupil plane,  $R$  is the radius of curvature of the converging wavefront in the exit pupil,  $k=2\pi/\lambda$ , and  $\epsilon_0$  is the amplitude of the electric field in the exit pupil (assuming uniform illumination).

If the effects of aberration are taken into account, in general, the wavefront in the exit pupil can be written as

$$\epsilon_{ab} = \epsilon(x_e, y_e) \text{EXP}[ik\phi(x_e, y_e)] \quad (3-3)$$

The parameter  $\phi$  is the aberration function and it completely describes the aberrations produced by the optical system. For the perfect optical system which introduces no aberrations, the parameter  $\phi=0$  (Ref 10:5).

The Strehl ratio is a parameter commonly used as a measure of the quality of an optical system. In the absence of aberrations the intensity is a maximum at the Gaussian image point. When aberrations are present this will, in general, no longer be the case and the point of maximum intensity is called the diffraction focus. In general

there may be more than one diffraction focus but if aberrations are sufficiently small, the diffraction focus is unique. The Strehl ratio is the ratio of the intensity at the diffraction focus in an aberrated system to the intensity at the Gaussian focus in an unaberrated system (Ref 4:461). It can be shown that for small aberrations the Strehl ratio,  $i(P)$ , can be approximated by

$$i(P) = 1 - k^2 (\overline{\phi^2} - \bar{\phi}^2) \quad (\text{Ref 4:464}) \quad (3-4)$$

In this equation  $\bar{\phi}^2$  is the square of the average wavefront deviation and  $\overline{\phi^2}$  is the average of the square of the wavefront deviation. The quantity in parentheses is the mean square wavefront deviation ( $\phi_{\text{rms}}^2$ ).

The Strehl ratio approximation indicates that the fractional intensity at the Gaussian focus,  $i(P)$ , is reduced from its optimum value of 1 by the quantity  $k^2$  times the mean square value of the wavefront aberration, where  $k$  is, as usual, defined as  $2\pi/\lambda$ . For an optical system with a Strehl ratio of unity, no greater peak intensity can be obtained by adjusting the components nor specifications within the optical system. This approximation is not meaningful for small values of the Strehl ratio ( $i < .1$ ) because for those cases the assumptions used to derive the equation are not valid.

Zernike Polynomials. The function  $\phi$  is used to describe the deviation of a given wavefront from a perfectly spherical one. For the ideal case where there is no aberration,  $\phi = 0$  and the intensity distribution from

a circular aperture is described by equation (3-1). For the more difficult cases where  $\phi$  is not zero, the problem arises to determine the impact of a non-zero aberration function on the intensity. For the case of a circular exit pupil, Zernike polynomials can be used.

Zernike polynomials are a set of functions orthogonal over the unit circle. By using these functions, any smooth aberration,  $\phi$ , can be uniquely represented by series sums of these functions. Zernike polynomials are the logical choice for this application because specific terms in the Zernike polynomial expansion can be related to the conventional Seidel aberrations.

The aberration function depends upon position within the exit pupil and is therefore a function of two variables.

$$\phi(x_e, y_e) = \sum_{nl} V_n^l(x_e, y_e) \quad (3-5)$$

The term  $V$  is the Zernike polynomial. The Zernike polynomial can be written in polar coordinates as

$$V_n^l(x, y) = R_n^l(\rho) e^{il\theta} \quad (3-6)$$

where  $x = \rho \sin\theta$  and  $y = \rho \cos\theta$ . The following restrictions apply to the indices of  $V$  and  $R$ :

$n, l$  integers

$n \geq |l|$

$n - |l| = \text{an even integer}$  (Ref 4:464).

The polynomials  $R_n^1(\rho)$  are called the Zernike circle or radial polynomials.

If  $\phi(\rho, \theta)$  is expanded in Zernike circle polynomials using equations (3-5) and (3-6) with the given restrictions on the indices of the circle polynomials

$$\begin{aligned} \phi(\rho, \theta) = & A_{00}R_0^0(\rho) \\ & + A_{01}R_0^1(\rho)e^{i\theta} \\ & + A_{0-1}R_0^{-1}(\rho)e^{-i\theta} \\ & + A_{22}R_2^2(\rho)e^{2i\theta} \\ & + A_{2-2}R_2^{-2}(\rho)e^{-2i\theta} \\ & + A_{20}R_2^0(\rho) \end{aligned} \quad (3-7)$$

A table of expanded Zernike circle polynomials is included as Appendix IV.

$$i(P) = 1 - \frac{K^2}{2} \sum \sum A_{nm}^2 / (n+1) \quad (3-8)$$

This states explicitly that the Strehl ratio can be calculated from the coefficients of the Zernike circle polynomial expansion. This, once again, is contingent upon the small aberration assumption made earlier.

Aberration Balancing. Often one objective in designing a lens system is to maximize the intensity in the focal plane. This is done by introducing carefully controlled aberrations to reduce the effects of other unwanted aberrations. A trade-off, however, does exist between adding some aberrations and reducing others. The use of Zernike circle

polynomials helps simplify this balancing process.

As an example, consider the case of spherical aberration, characterized by rays converging in several planes other than the focal plane. The distance between the Gaussian focal plane and the plane in which a given ray focuses is dependent upon the zone in which the ray enters the system. For zones farther away from the optical axis, a ray's length is shorter than for zones closer to the optical axis. Spherical aberration can be minimized by inserting an aperture to limit the zones to the paraxial region but in some cases this may not be practical. Also by shifting the position of the focal plane to a more central position (e.g. the circle of least confusion), the spherical aberration can be reduced. Also by the addition of controlled amounts of other aberrations, the unwanted spherical aberration can be reduced.

As an example, assume a given optical system has a known amount of sixth order spherical aberration;

$$\phi = a_6 \rho^6$$

The Zernike circle polynomial representing the aberration must necessarily consist of the  $R_6^0$  polynomial to include the  $\rho^6$  without a cosine dependence. The remaining terms must be cancelled by the inclusion of other appropriate Zernike circle polynomials of lower order (Ref 4:468).

With this in mind

$$\begin{aligned}
\phi = & A_{60}(20\rho^6 - 30\rho^4 + 12\rho^2 - 1) \\
& + A_{40}(6\rho^4 - 6\rho^2 + 1) \\
& + A_{20}(2\rho^2 - 1) + A_{00}
\end{aligned}
\tag{3-9}$$

The condition  $\phi = a_6 \rho^6$  requires that the coefficient of the first polynomial ( $A_{60}$ ) equal  $a_6/20$ . This in turn adjusts the coefficients of the lower order terms in the first polynomial as follows:

$$-3a_6/2 \rho^4 + 3a_6/5 \rho^2 + a_6/20$$

The second polynomial is included to nullify the  $\rho^4$  term in the  $R_6^0$  polynomial. In this case

$$6A_{40}\rho^4 = 3a_6/2 \rho^4$$

requiring that  $A_{40} = a_6/4$ .

This, in turn, adjusts the remaining terms in the  $R_4^0$  polynomial as follows:

$$-3a_6/2 \rho^2 + a_6/4$$

This term is added to the surviving terms of the  $R_6^0$  polynomial to yield

$$-9a_6/10 + a_6/5.$$

The third polynomial is included to nullify the  $\rho^2$  term in the  $R_4^0$  polynomial which requires

$$9a_6/20 - A_{20}.$$

This leaves as the surviving term

$$-a_6/4$$

requiring  $A_{00} = a_6/4$  to nullify it. Using equation (3-8), the Strehl ratio is given by

$$i(P) = 1 - \frac{k^2}{2} [a_6^2/16 + 1/3 \ 81a_6^2/400 + 1/5 \ a_6^2/16].$$

Thus the Strehl ratio can be calculated at a given wavelength for a known value of  $a_6$  (Ref 10:35).

By eliminating certain terms in equation (3-9) the value of the Strehl ratio can be improved. This is done by introducing other aberrations, for example  $A_{40}$  of  $-a_6/4$  and  $A_{20}$  of  $-9a_6/20$  will eliminate the corresponding terms in equation (3-8) with the end result being an increase in  $i(P)$  (Ref 10:36).

Tolerance Conditions for Primary Aberrations. In optical design the question of how much of each type of aberration can be tolerated without seriously degrading the image naturally arises. For the case of an optical system with a circular aperture imaging a bright point object, diffracted image will be the familiar Airy pattern. The presence of aberrations causes a reduction in intensity of the central maximum, the halfwidth of the maximum remains unchanged, and more light appears in the outer rings (Ref 12:206).

It was first found by Rayleigh in 1879 that when a system suffers from primary spherical aberration of such

an amount that the wavefront in the exit pupil departs from the spherical reference wavefront by less than one quarter of a wavelength, the reduction in intensity at the diffraction focus is less than 20 percent (Ref 4:468). In the absence of aberrations, the intensity is a maximum at the Gaussian focus. When aberrations are present, the point of maximum intensity is the diffraction focus (Ref 4:461). Later it was found that if this quarter wavelength limit were adhered to, the image is also not seriously degraded in the presence of other aberrations. This result became known as the Rayleigh quarter wave limit. This, however, is a coarse guideline and must be used in conjunction with a knowledge of the application to which the system will be put. When the condition  $\phi_{\max} = \lambda/4$  is applied to aberrations of different types, a variety of values for the intensity at the diffraction focus are obtained.

It is more appropriate to consider each individual aberration and to determine a tolerance for each one to yield a given intensity level at the diffraction focus. Criteria of this type were considered by Marechal in 1947 (Ref 4:469). As was stated earlier, when aberrations are sufficiently small

$$i(P) = 1 - k^2 (\overline{\phi^2} - \bar{\phi}^2).$$

The quantity in parentheses is the mean square deviation of the aberrated wavefront from a spherical reference

wavefront ( $\phi^2_{\text{rms}}$ ). If the intensity of 80 percent of the Gaussian intensity is used as the criterion,

$$i(P) \geq 0.8$$

Substituting a Strehl ratio of 0.8 into the above equation,

$$\phi^2_{\text{rms}} > \lambda/14.0496$$

This is equivalent to saying that the root mean square departure of the wavefront from the reference sphere centered on the diffraction focus shall not exceed the value of  $\lambda/14$ .

This leaves two remaining items to be considered. First, the location of the diffraction focus is still in question, and secondly, tolerance conditions for spherical aberration, coma, and astigmatism must be considered. Since field curvature and distortion act to shift the focus, and not strictly to degrade the quality of the image, tolerances for those cases will not be considered.

In terms of the Zernike circle polynomials, each primary aberration can be represented in the form

$$\phi = \epsilon_{nm} A_{1nm} R_n^m(\rho) \cos m\theta \quad (3-10)$$

where  $\epsilon_{nm} = 1/1.414$  for  $n=0, m \neq 0$   
 $= 1$  otherwise.

Zernike circle polynomials are shown in Figure 3-1 where

the appropriate polynomial is expanded (Ref 4-470).

<u>Aberration</u>	<u>l</u>	<u>n</u>	<u>m</u>	<u>Representation</u>
Spherical	0	4	0	$1/1.414 A_{040} (6\rho^4 - 6\rho^2 + 1)$
Coma	0	3	1	$A_{031} (3\rho^3 - 2\rho) \cos \theta$
Astigmatism	0	2	2	$A_{022} \rho^2 (2\cos^2 \theta - 1)$
Field Curv.	1	2	0	$1/1.414 A_{120} (2\rho^2 - 1)$
Distortion	1	1	1	$A_{111} \rho \cos \theta$

Figure 3-1. Zernike Representation of Primary Aberrations

It is appropriate now to include the displacement theorem as stated by Born and Wolf:

"The addition to an aberration function of a term  $H\rho^2 + K\rho \sin \theta + L\rho \cos \theta + M$  where H, K, L, and M are constants of order  $\lambda$  results in no change in the three dimensional intensity distribution near focus, apart from a displacement of distribution as a whole in accordance with the equations

$$z' = z + (2R/a)^2 H; \quad x' = x + (R/a)K; \quad y' = y + (R/a)L'$$

These three equations give the location of the diffraction focus with respect to the Gaussian focus.

In Figure 3-2 the primary aberrations are given in terms of the wavefront aberration, the coefficients being

primed to avoid confusion with the Zernike circle polynomial coefficients (Ref 4:470).

<u>Aberration</u>	<u>l n m</u>	<u>Representation</u>
Spherical	0 4 0	$A'_{040}\rho^4$
Coma	0 3 1	$A'_{031}\rho^3 \cos \theta$
Astigmatism	0 2 2	$A'_{022}\rho^2 \cos^2 \theta$
Field Curv.	1 2 0	$A'_{120}\rho^2$
Distortion	1 1 1	$A'_{111}\rho \cos \theta$

Figure 3-2. Wavefront Aberrations

If the shift in focus is given by

$$6/1.414 A_{040} = A'_{040} = H \quad (3-11)$$

$$K = L = 0.$$

Substituting these values into the equations of the displacement theorem determines the diffraction focus with respect to the Gaussian focus.

The problem of determining the tolerance for a given aberration remains. Using equation (3-8) and a Strehl ratio of 0.8 as a lower limit, the following equation results:

$$1 - k^2/2 A_{1nm}^2 / (n+1) > 0.8$$

Which can be reduced to  $A_{1nm} = \lambda n+1/9.935$  yielding a

value of  $.225 \lambda$  for  $A_{040}$ . Using equation (4-14) the Zernike polynomial coefficient is converted to the wavefront aberration coefficient value  $A'_{040} = .955 \lambda$ . This states that the maximum deviation of the wavefront from the Gaussian reference sphere cannot exceed  $.955 \lambda$  to maintain a Strehl ratio of 0.8. Coma and astigmatism tolerances are determined similarly.

Appendix IV

Zernike Circle Polynomials

Zernike Circle Polynomials  $R_n^m(\rho)$  for  $n, m \leq 8$

<u>m</u>	<u>n</u>	<u><math>R_n^m</math></u>
0	0	1
0	2	$2\rho^2 - 1$
0	4	$6\rho^4 - 6\rho^2 + 1$
0	6	$20\rho^6 - 30\rho^4 + 12\rho^2 - 1$
0	8	$70\rho^8 - 140\rho^6 + 90\rho^4 - 20\rho^2 + 1$
1	1	$\rho$
1	3	$3\rho^3 - 2\rho$
1	5	$10\rho^5 - 12\rho^3 + 3\rho$
1	7	$35\rho^7 - 60\rho^5 + 30\rho^3 - 4\rho$
2	2	$\rho^2$
2	4	$4\rho^4 - 3\rho^2$
2	6	$15\rho^6 - 20\rho^4 + 6\rho^2$
2	8	$56\rho^8 - 105\rho^6 - 60\rho^4 - 10\rho^2$
3	3	$\rho^3$
3	5	$5\rho^5 - 4\rho^3$
3	7	$21\rho^7 - 30\rho^5 + 10\rho^3$
4	4	$\rho^4$
4	6	$6\rho^6 - 5\rho^4$

Appendix IV (continued)

$m$	$n$	$R_n^m$
4	8	$28\rho^8 - 42\rho^6 + 15\rho^4$
5	5	$\rho^5$
5	7	$7\rho^7 - 6\rho^5$
6	6	$\rho^6$
6	8	$8\rho^8 - 7\rho^6$
7	7	$\rho^7$
8	8	$\rho^8$

Appendix V

Basic Program Listing

```
10 REM ** PROGRAM TO CALCULATE PARAMETERS FOR BEAM **
20 REM ** EXPANDER **
30 REM * ITERATIVELY SPECIFY F3 *
40 LPRINT "      CV1      CV2      CV3      D2      D3      "
50 LPRINT;LPRINT
60 DEFDBL A-H
70 DEFDBL J-Z
80 FOR I=100 TO 500 STEP 10
90 F3 = I
100 F2 = F3/-.8
110 D3 = .2*F2
120 F1 = F2/8
130 D2 = F1-F2
140 CV1 = 1/(2*F1)
150 CV2 = 1/(2*F2)
160 CV3 = 1/(2*F3)
170 REM *** CALCULATE DECENTER PARAMETERS ***
180 DEC2 = D2*.0348994967
190 DEC3 = D3*.0871557427
200 LPRINT USING " _ #.#####^";CV1, CV2, CV3, D2, D3, DEC2, DEC3
210 NEXT I
```

## VITA

Donald J. Tipple was born on 28 June 1954 in Saranac Lake, New York. He graduated from high school in 1972 and attended Hartwick College, Oneonta, New York from which he earned the degree of Bachelor of Arts in Physics in May 1976. Upon graduation, he applied his talents doing calibration assessments of radiological equipment for Radiological Physics Associates. In August 1977 he entered the Air Force and received his commission from Officer Training School in November. He was assigned to the Air Force Weapons Laboratory, EMP Test Division, Kirtland AFB, New Mexico as a Nuclear Effects Test Officer. There he did EMP survivability and vulnerability testing of several DoD systems. He was selected to attend the Air Force Institute of Technology in March of 1982 and entered the school of engineering in May 1982 with the class of GEP-83D.

UNCLASSIFIED

SECURITY CLASSIFICATION OF THIS PAGE

REPORT DOCUMENTATION PAGE

1a. REPORT SECURITY CLASSIFICATION <b>UNCLASSIFIED</b>		1b. RESTRICTIVE MARKINGS	
2a. SECURITY CLASSIFICATION AUTHORITY		3. DISTRIBUTION/AVAILABILITY OF REPORT Approved for public release; distribution unlimited	
2b. DECLASSIFICATION/DOWNGRADING SCHEDULE		4. PERFORMING ORGANIZATION REPORT NUMBER(S) AFIT/CEP/PH/83D-14	
4. PERFORMING ORGANIZATION REPORT NUMBER(S)		5. MONITORING ORGANIZATION REPORT NUMBER(S)	
6a. NAME OF PERFORMING ORGANIZATION School of Engineering	6b. OFFICE SYMBOL (If applicable) AFIT/ EN	7a. NAME OF MONITORING ORGANIZATION	
6c. ADDRESS (City, State and ZIP Code) Air Force Institute of Technology Wright-Patterson AFB, Ohio 45433		7b. ADDRESS (City, State and ZIP Code)	
8a. NAME OF FUNDING/SPONSORING ORGANIZATION	8b. OFFICE SYMBOL (If applicable)	9. PROCUREMENT INSTRUMENT IDENTIFICATION NUMBER	
8c. ADDRESS (City, State and ZIP Code)		10. SOURCE OF FUNDING NOS.	
11. TITLE (Include Security Classification) See Box 19		PROGRAM ELEMENT NO.	PROJECT NO.
		TASK NO.	WORK UNIT NO.
12. PERSONAL AUTHOR(S) Donald J. Pipple, B.A., Capt, USAF			
13a. TYPE OF REPORT MS Thesis	13b. TIME COVERED FROM _____ TO _____	14. DATE OF REPORT (Yr., Mo., Day) 1983 December	15. PAGE COUNT 115
16. SUPPLEMENTARY NOTATION			
17. COSATI CODES		18. SUBJECT TERMS (Continue on reverse if necessary and identify by block number)	
FIELD	GROUP	SUB. GR.	
20	06		
19. ABSTRACT (Continue on reverse if necessary and identify by block number)			
Title: COMPUTER AIDED GEOMETRICAL OPTICS DESIGN			
Thesis Chairman: John H. Erkkila, Lieutenant Colonel, USAF			
Approved for public release: LAW AFR 100-10 <i>[Signature]</i> JOHN E. WOLVER Dean for Research and Professional Development Air Force Institute of Technology (AFIT) Wright-Patterson AFB OH 45433			
20. DISTRIBUTION/AVAILABILITY OF ABSTRACT UNCLASSIFIED/UNLIMITED <input checked="" type="checkbox"/> SAME AS RPT. <input type="checkbox"/> DTIC USERS <input type="checkbox"/>		21. ABSTRACT SECURITY CLASSIFICATION UNCLASSIFIED	
22a. NAME OF RESPONSIBLE INDIVIDUAL John H. Erkkila, Lt Col, USAF	22b. TELEPHONE NUMBER (Include Area Code) 513 255-5187	22c. OFFICE SYMBOL AFIT/EN	

The FALCON optical design and evaluation computer program was examined and applied to two efforts. The first effort involved the evaluation of a Cooke triplet and manual verification of some of the code's results. The second effort was the design of a beam expander, the function of which is to expand and square a high aspect ratio rectangular laser beam. The system uses a single spherical mirror and two cylindrical mirrors to produce the desired output. A brief discussion of the diffraction theory of aberrations and aberration balancing gives some of the basis upon which the FALCON code is constructed.

**END**

**FILMED**

**10-84**

**DTIC**